GENERAL ATOMIC

GA-A14381
UC-77

GAS TURBINE HTGR PROGRAM

QUARTERLY PROGRESS REPORT FOR THE PERIOD ENDING MARCH 31, 1977

by
PROJECT STAFF

Prepared under
Contract EY-76-C-03-0167
Project Agreement No. 46
for the San Francisco Operations Office
U.S. Energy Research and Development Administration

GENERAL ATOMIC PROJECT NO. 3227 DATE PUBLISHED: APRIL 1977

ABSTRACT

This report describes work on the Gas Turbine High-Temperature Gas-Cooled Reactor (GT-HTGR) Program, Contract EY-76-C-03-0167, Project Agreement No. 46, performed during the period January 1, 1977, through March 31, 1977.

The report describes early conceptual studies of a 2-loop intercooled 3000 MW(t) plant which, together with existing conceptual designs of a 3-loop intercooled 3000 MW(t) plant, can be compared with designs being studied by the HHT Project. The objective of this effort is to determine a basis for a common development program and demonstration plant.

The 2-loop intercooled design is compared to the 3-loop nonintercooled 300 MW(t) reference design of General Atomic Company. The turbomachine increased in rating from 400 to 620 MW(e) and in length from 37 to 52 ft. The larger heat exchangers required caused the PCRV diameter to increase from 118 to 128 ft and the height from 111 to 125 ft. The system pressure losses increased from 7.15 to 10.60%. The plant efficiency increased from 39.6 to 41.2%. Initial indications are that the increase in efficiency roughly balances the increased cost of the reactor turbine system.

CONTENTS

FIGURES

FIGURES (Continued)

TABLES

TABLES (Continued)

1. INTRODUCTION AND SUMMARY

This report describes progress on the direct cycle Gas Turbine High Temperature Gas-Cooled Reactor (GT-HTGR) Program, Contract EY-76-C-03-0167, Project Agreement No. 46 for the period January 1, 1977, through March 31, 1977. The Project Agreement No. 46 program is comprised of a conceptual design task and a materials task. Covered in this report are General Atomic Company (GA) conceptual design studies on the configuration and incentives for direct cycle power plants. Previous results from the ERDA-sponsored GT-HTGR program are described in Refs. 1, 2, and 3.

The progress on the Gas Turbine and Advanced HTGR Materials Screening task for the period October 1, 1976, through March 31, 1977 is reported separately in Ref. 4. The collaborative creep-corrosion screening testing at CIIR is managed by Kernforschungsanlage (KFA), Jülich, Germany and is partially supported by ERDA. The testing program has completed 13,000 hr, and detailed metallurgical analyses of specimens exposed for 10,000 hr have been documented.

Creep curves, weight gain data, residual tensile properties, corrosion depths (oxidation and carburization) and microstructural changes have been obtained on many of the 25 candidate alloys tested in air and simulated reactor helium (with controlled impurities) at 650° and 900°C. Results to date indicate no significant degradation in creep properties of the baseline vacuum-cast turbine blade/vane superalloys; candidate casing/ducting wrought solid-solution, nickel alloys, however, have exhibited significant carburization, with attendant reduction in creep properties, at 900°C. The resistance of nickel alloys to carburization has been correlated to the composition and protective nature of the oxide film, with the presence of titanium in the film being particularly beneficial.

In testing at GA, vacuum evaporation aging tests at 800° to 900°C have been terminated after 10,000 hr. Evaporation of alloying elements (Cr, Mn) was determined to be significant at 900°C but not at 800°C. An experimental parametric study to define tolerable levels of helium impurities for specific classes of alloys has been initiated after design and construction of a test rig that can furnish six different impurity compositions simultaneously.

The conceptual design studies during the quarter are related to objectives that include joint international determination of the major design concepts and parameters of GT-HTGR plants and definition of common or shared international development programs. The current U.S. reference design for a commercial-type plant incorporates multiple (3 or 4 depending on output) nonintercooled, 60-Hz power conversion loops, each rated at 1000 MW(t) input and 400 MW(e) output. The current European HHT reference design (for 50 Hz) incorporates a single, intercooled 1200 MW(e) turbomachine and two parallel heat exchanger trains, with a 3000 MW(t) core. Although the U.S. and European plant reference designs are suitable and competitive for their respective applications, differences in generating frequency, and application factors such as average atmospheric temperature lead to problems in joint adoption of either reference design. Thus, GA, together with United Technologies Corporation on the turbomachinery, has undertaken conceptual design studies of a 2-loop plant incorporating intercooled power conversion loops, each rated at 1500 MW(t) input and 620 MW(e) output, to assess its technical feasibility and economic competitiveness.

The conceptual design of the 2-loop intercooled plant is compared on the basis of a 3000 MW(t) nominal rating to a reference plant (3-loop nonintercooled), with respect to the performance parameters listed in Table 1-1.

TABLE 1-1
PERFORMANCE COMPARISON OF SELECTED GT-HTGR DESIGNS

Plant	3-Loop Nonintercooled	2-Loop Intercooled
Design status	Reference design with optimized cycle parameters	Initial conceptual design
Reactor thermal rating, MW(t)	3000	3000
Number of loops	3	2
Cycle type	Nonintercooled	Intercooled
Plant type	Integrated	Integrated
Heat rejection	Dry cooled	Dry cooled
Turbine inlet temperature, °C (°F)	850 (1562)	850 (1562)
Loop rating, MW(t)	1000	1500
Turbomachine rating, MW(e)	400	620
Turbomachine orientation	Delta	Chordal
PCRV diameter, m (ft)	36 (118)	39 (128)
PCRV height, m (ft)	34.1 (111)	38.1 (125)
System pressure losses ($\Delta P/P$) %	7.15	10.60
Plant power, MW(e)	1186.5	1237
Plant efficiency, %	39.55	41.23

GA-A14381

It is believed that some improvement in the 2-loop intercooled plant efficiency to the range of 42-43% is possible with more design study and optimization, particularly through attention to the turbomachines. However, the Table 1-1 information shows that the introduction of intercooling does not realize all its theoretical improvements in efficiency, because of additional loop pressure losses and constraints on turbomachinery design. The presently calculated efficiency of 41.2% compares favorably with HHT predictions. Detailed cycle performance is presented in Section 2 of this report.

The arrangement of the 2-loop turbomachines in the prestressed concrete reactor vessel (PCRV) has the centerline along a chord of the PCRV, unlike the HHT design, which has a radial layout. The layout objectives have been to minimize PCRV diameter, which is dictated by the line running through the core and the recuperator. The introduction of the intercooled cavity leads to displacement of the turbomachinery, so that azimuthal symmetry cannot be maintained. These constraints and other factors affecting the primary system layout are described in Section 3.

United Technologies Inc. has performed conceptual design studies for the 60 Hz, 2-loop turbomachine and has concluded that a turbine rotor blade life of 40 years without blade cooling is feasible. This conclusion is consistent with their previous observations on a 1333 MW(t) nonintercooled machine design that has approximately the same mass flow. The initial design studies were based on a 3-bearing machine (an additional bearing between high- and low-pressure compressor). However, later calculations not reported here, indicate that a 2-bearing system may be possible, which would reduce the machine length and hence some PCRV constraints. Details of the turbomachine studies are given in Section 4.1.

Conceptual designs of the recuperator, precooler, and intercooler have been performed and are described in Section 4.2. The recuperator is a very large heat exchanger that is pushing near the limits of manufacturability and transportability. Additional work is needed to establish the most suitable design within feasible manufacturing technology. Pressure losses in the heat exchangers and in the ducting are described in Section 4.

2. CYCLE PARAMETERS AND PERFORMANCE

2.1 CYCLE DESCRIPTION

The intercooled cycle differs from the nonintercooled cycle in only one major respect: With the intercooled cycle, helium is compressed in two stages rather than in a single stage. Since the helium is cooled between the compression stages (removing the heat of compression), the term, intercooled, is used to characterize the cycle.

Figure 2-1 shows the cycle configuration and gives cycle conditions. This diagram is distinguished from the nonintercooled one by the presence of two compressors separated by a water-to-helium intercooler. The functions of the reactor, turbine, recuperator, and precooler remain the same in this cycle as they are in the nonintercooled cycle.

The turbine drives both compressors; all three components of the turbomachine are located on a single shaft. Heat is transferred from the low-pressure side of the recuperator to the high-pressure side to recover the thermal energy present at the turbine exhaust, the same as in the nonintercooled design.

2.2 CYCLE PERFORMANCE

The theoretical advantage, with respect to cycle efficiency, of the intercooled design is immediately apparent: The intercooler reduces the average temperature at which helium is compressed. This reduces the power necessary for compression, which increases the net power available from the turbine, and thereby increases net plant output. Or, by analogy to a Carnot cycle, the average temperature at which heat is rejected from the cycle (in the precooler and in the intercooler) is reduced, thereby increasing cycle efficiency.

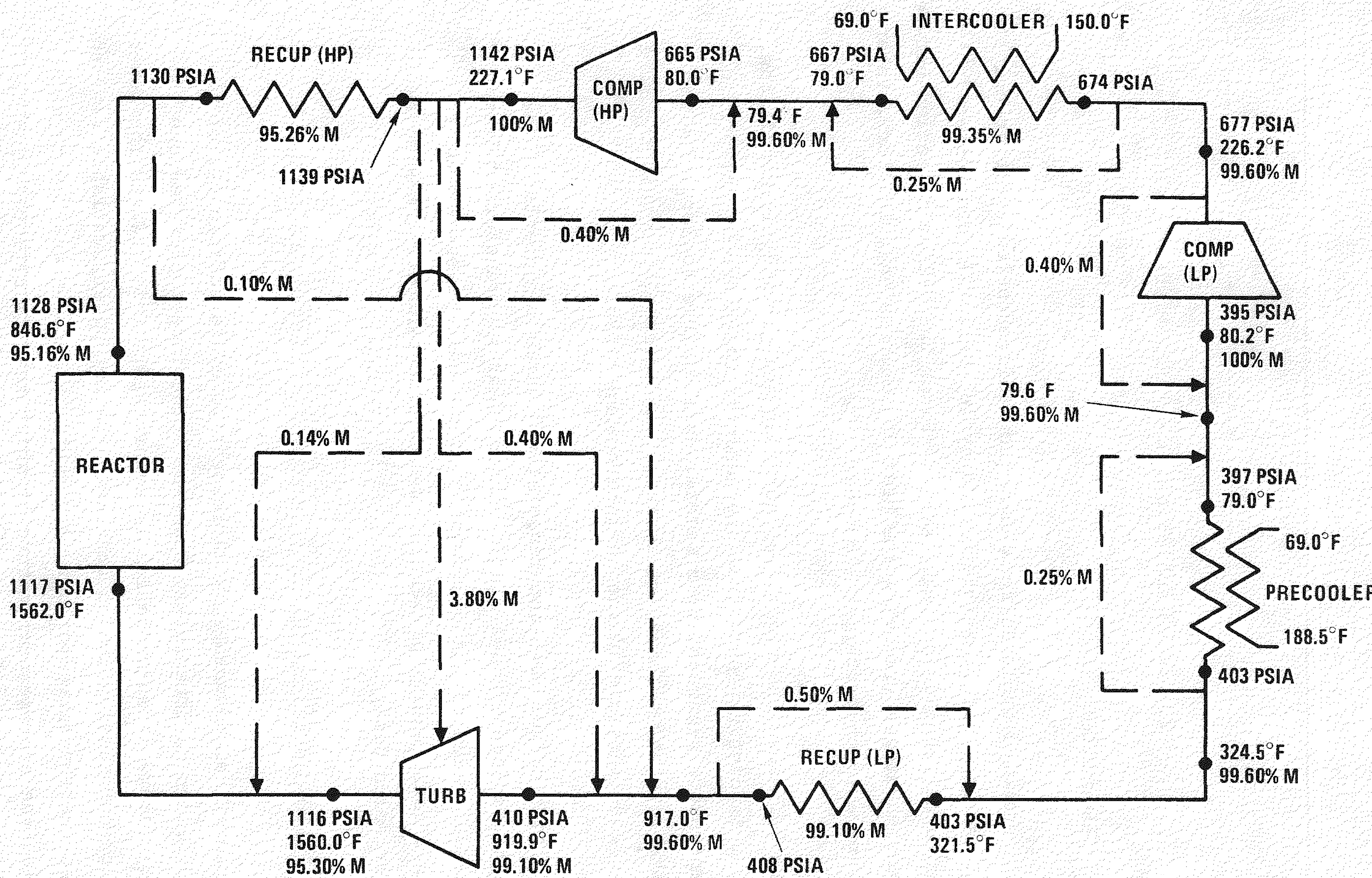

M = REFERENCE FLOW RATE = 12,039,000 LB/HR

GA-A14381

Fig. 2-1. Cycle diagram of 2-loop intercooled gas turbine HTGR plant with dry cooling (ISO rating)

There are practical limitations to achieving all the theoretical gains in efficiency, as this study has shown. General Atomic has adopted two loops for a 3000 MW(t) reactor for the intercooled cycle, versus three loops for the nonintercooled cycle. This is a reasonable approach from a PCRV layout standpoint, because the numbers of heat exchangers which must be fit into the PCRV remains the same: three per loop times two loops for the intercooled cycle and two per loop times three loops for the nonintercooled cycle. However, this means that the plant helium flow must be passed through only two loops in parallel instead of three. In addition, with the introduction of an extra compressor stage and an extra heat exchanger in each loop, the helium sees more components in the circuit. The effect of these changes is to significantly increase the helium pressure losses, which has a large adverse effect on cycle efficiency.

There are other differences affecting cycle performance in comparison to the nonintercooled plant, e.g., turbine and compressor efficiencies and turbine cooling flows. These, however, tend to be detail design differences and not fundamental cycle differences.

Major design parameters are given in Table 2-1. Cycle conditions are shown in Fig. 2-1. Heat balance parameters are provided in Table 2-2. In Fig. 2-1 the main helium flow is shown (in solid lines), and leakage and cooling flows are shown (in dashed lines).

The intercooled GT-HTGR cycle efficiency is 41.23%. This estimate is consistent with and comparable to the 39.55% efficiency estimate for the nonintercooled configuration. (These figures reflect the fact that the nonintercooled plant has benefited from extensive optimization work, while the intercooled plant has not.)

TABLE 2-1
MAJOR PARAMETERS AND PERFORMANCE RESULTS
(INTERCOOLED CYCLE)

Item	Value
Reactor outlet temperature, °C (°F)	850 (1562)
Total compressor pressure ratio	3.00
Individual compressor pressure ratios (each)	1.732
Minimum cycle helium temperature, °C (°F)	26.1 (79)
Compressor inlet temperature, °C (°F)	26.7 (80)
Maximum cycle helium pressure, MPa (psia)	7.93 (1150)
Recuperator effectiveness	0.898
Total system pressure loss parameter	1.1114
Equivalent total $\Delta P/P$, %	10.0
Turbine polytropic efficiency, %	90.6
isentropic efficiency, %	92.2
High-pressure compressor polytropic efficiency, %	91.2
isentropic efficiency, %	90.2
Low-pressure compressor polytropic efficiency, %	91.7
isentropic efficiency, %	90.8
Disk cooling flow, %	3.8
Generator efficiency, %	98.8
Helium mass flow rate (through compressors), kg/sec (lb/hr)	1516.9 (12,039,000)
Reactor rating, MW(t)	3000
Net electrical output, MW(e)	1237
Plant efficiency, %	41.23

GA-A14381

TABLE 2-2
HEAT BALANCE

	Plant Output (MW)	Primary System (MW)
Reactor power		+3000
Primary system heat loss		(18.9)
Turbine gross power	2556.4	(2556.4)
Low-pressure compressor gross power	(640.2)	+640.2
High-pressure compressor gross power	(645.1)	+645.1
Heat rejected from precooler		(1068.5)
Heat rejected from intercooler		(641.3)
Bearing losses	(7.9)	
Generator losses	(15.3)	
Plant auxiliary power	(11.0)	
Net plant output	1236.9	
Primary system heat balance (error)		0.2

GA-A14381

3. INTERCOOLED PLANT CONFIGURATION

3.1 PRIMARY SYSTEM DEVELOPMENT

With the establishment of cycle parameters, as outlined in Section 2, conceptual design work of the major components was initiated and layout of the primary system configuration. In the past, several iterations were necessary to establish an arrangement that satisfied all of the design criteria (i.e., structural, safety, performance, cost, etc.). The plant configuration described in this section represents a second iteration (following component sizing, particularly the turbomachine), and it is apparent that further design refinements, which will be discussed briefly, are necessary to reduce the system pressure loss. In the limited time available for the study of a 2-loop intercooled plant, the following ground rules were observed:

1. Simplicity in the primary system was emphasized.

2. Component orientation for minimum PCRV size was established.

3. Gas flow path geometries, etc., were selected for minimum pressure loss.

4. Flexibility of configuration was emphasized, so that with minor modifications, warm-liner or cooled-liner approaches could be utilized.

5. Experience gained from the 3-loop nonintercooled reference plant was utilized to the maximum.

3.1.1 Equipment Orientation

Layout of the primary system is shown in Figs. 3-1, 3-2, and 3-3. From the plan view of the PCRV it can be seen that the two turbomachines are arranged in a semichordal configuration, the angle between the units essentially being controlled by the generator length. This orientation of the machines was favored, since it results in maximum utilization of the space within the vessel and perhaps enables a common generator cell to be considered. Until more definitive data is received, a standard (in the U.S.) generator was considered, with a water-cooled stator and a hydrogen-cooled rotor and gap. As before, to eliminate the hydrogen explosion hazard, the generators are isolated from the secondary containment. Adopting United Engineers & Constructors Co. recommendation (for the 3-loop plant), the generators have been moved farther away from the secondary containment, for the following reasons:

1. To position the electrical connections outside of the secondary containment

2. To facilitate overhead crane coverage for the steel hatch cover.

If an all water-cooled generator is available in the 720 MVA power size, the hydrogen explosion problem could be eliminated and the unit could be positioned within the secondary containment, with local cells being incorporated to minimize the diameter of the containment building. More attention to design is required in this area before the final solution can be identified.

The configuration shown in Figs. 3-1, 3-2, and 3-3 utilizes a conventional water-cooled liner with thermal barrier in the PCRV. With slight modifications to the primary system gas flow paths, either partial or full gas flow could be provisioned adjacent to the liner in the recuperator, precooler, and core cavities, (i.e., the warm liner approach). Limited studies were done of the orientation of the three vertical heat exchangers, to give

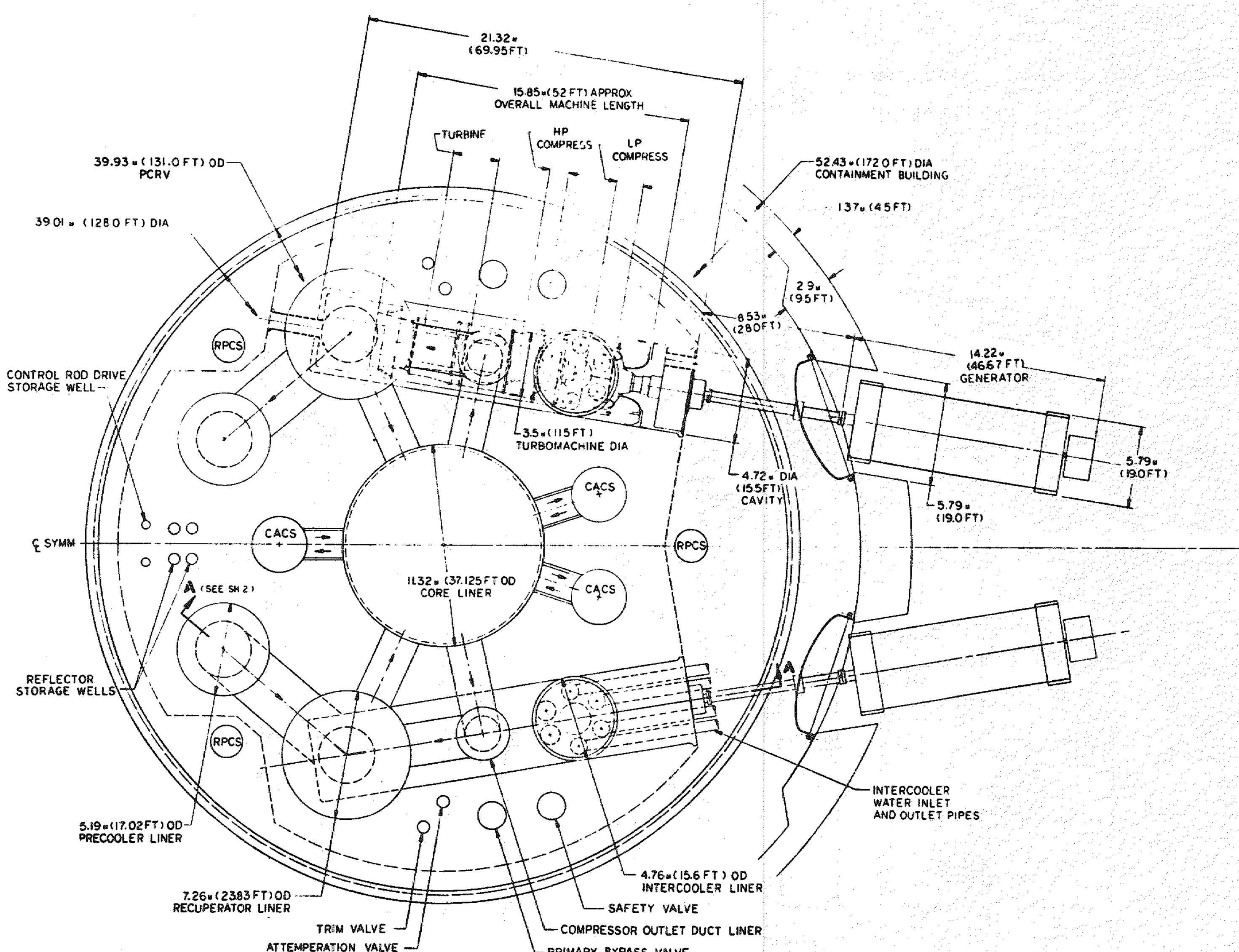

Fig. 3-1. Plan view of 2-loop intercooled plant

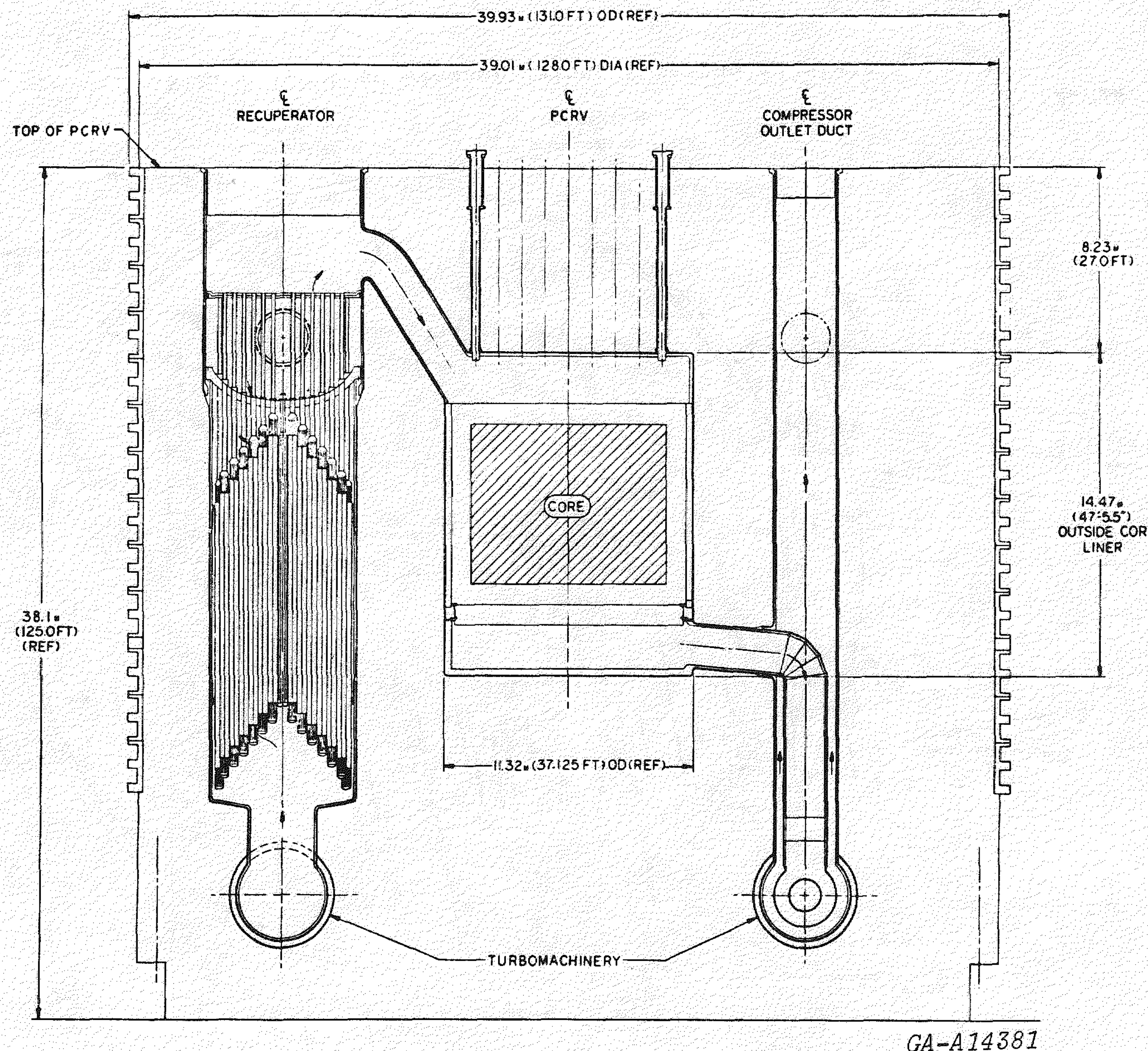

Fig. 3-2. Vertical section of 2-loop intercooled plant through core and power conversion loop

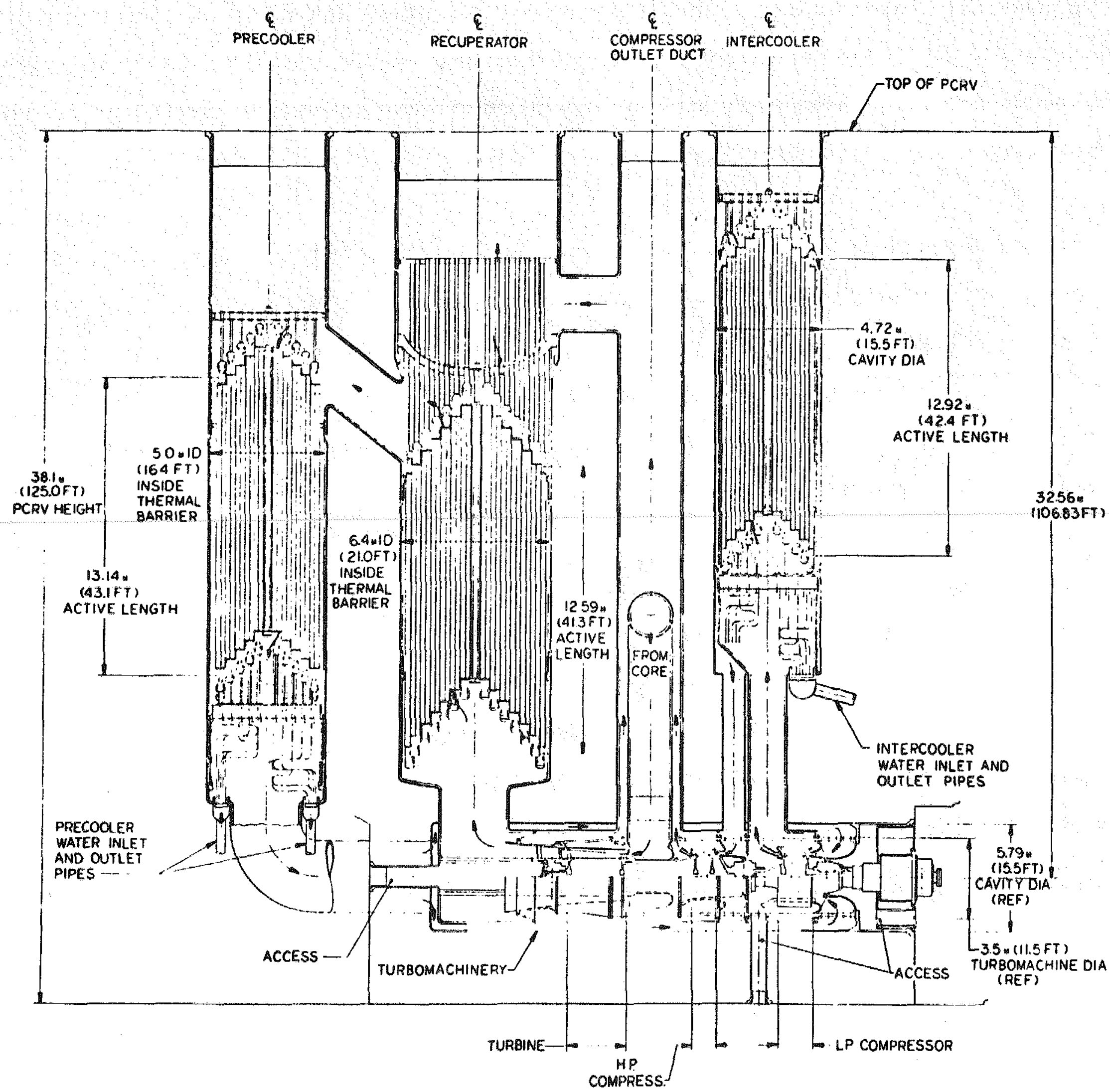

GA-A14381

Fig. 3-3. Vertical section of 2-loop intercooled plant through power conversion loop the simplest gas flow paths within the primary system. The configuration shown has the recuperator and intercooler mounted directly above the turbomachinery with the precooler off to one side, which results in a good gas flow path from the recuperator to the precooler through an annulus in the turbomachine cavity to the region of the LP compressor inlet.

As in previous PCRV layout studies, the diameter of the recuperator (in conjunction with the core cavity) was found to be the limiting factor controlling the PCRV diameter. The vessel diameter is 39 m (128 ft) (Fig. 3-2). The diameter of a single-domed support plate for the recuperator is near the upper limit possible with a forging made of ferritic material. A recuperator of this size must be assembled at the site, but tentative plans call for installation of the complete assembly in the vessel, using a system of hydraulic jacks. The height of the PCRV at 38.1 m (125 ft) is somewhat higher than the minimum, as determined by a summation of the core cavity height and top and bottom head thicknesses. This results from the large duct diameters associated with two loops (for low pressure loss) and the diameter constraint imposed on the recuperator (necessitating increased tube length). Because of the cost impact, further design work is required to minimize the vessel height.

The plan view of the PCRV (Fig. 3-1) shows 3 CACS units, each of 50% capacity. These have not been engineered and were included in the layout only to show that they can be accommodated in the 2-loop plant configuration.

From the plant layouts (Figs. 3-1, 3-2, and 3-3), it can be seen that emphasis has been placed on utilizing the turbomachine cavity for flow path boundaries. Although large circumferential seals are required (which have not been engineered), compartmentalizing the turbomachine cavity is a more viable approach than having a multiplicity of flanged joints, which would require remote actuation. With the flanged joint approach, the scroll and volute flow areas are restricted, which results in parasitic pressure losses that have an adverse effect on plant performance. The single turbine inlet duct, which is 1.74 m (5.7 ft) in diameter, is the only retractable duct in the turbomachine cavity. A condensed comparison of the main features of the turbomachinery for the nonintercooled and intercooled plant variants is shown in Table 3-1.

At the stage of the plant conceptual design shown in Figs. 3-1, 3-2, and 3-3, the heat exchangers lack detailed design definition; they are sized to support the primary system design effort, thus the selected solutions are not regarded as optimum. The conceptual designs of the precooler and intercooler are based upon the utilization of plain tubes, as opposed to the internally-finned geometries in the previous (3-loop, Delta) designs. The intercooler structure embodies a shroud assembly for transporting the cooled gas back down into the HP compressor, which creates the need for a thermal barrier in this cavity. The diameters sizes of both the precooler and intercooler enable these exchangers to be completely fabricated and assembled at the factory and transported to the site.

All three heat exchangers are designed to utilize a compact headering arrangement. The conical subheadering approach is used, but it is recognized that elastically deformed tube approaches are equally applicable. The recuperator contains integral return tubes, and a seal and bellows arrangement is included to account for differential thermal expansions (i.e., return tube-to-module). To accommodate differential expansion in the lead tubes (above the top support plane), a floating flat plate has been included, since this structure operates with a very small pressure differential. Although there are other top subheadering approaches (i.e., a drum assembly), the conical variant was selected for the following reasons:

1. To accommodate straight return lead tubes

2. To eliminate a multiplicity (one per module) of piston ring seals

3. To make maximum use of the PCRV cavity

TABLE 3-1
GAS TURBINE HTGR TURBOMACHINE COMPARISON

Plant	3-loop Nonintercooled	2-loop Intercooled
Turbomachines per plant	3	2
Machine thermal rating, MW(t)	1000	1500
Machine rating, MW(e)	400	620
Machine type	Single-shaft	Single-shaft
Number of turbine inlets	One	One
Turbine inlet temperature, °C (°F)	850 (1562)	850 (1562)
Compressor pressure ratio	2.50	3.0 (1.732/1.732)
Turbine blading	Uncooled, nickel-base alloy	Uncooled, nickel-base alloy
Rotor construction	Welded	Welded
Blading life, hr	280,000	280,000
Compressor efficiency, %	89.8	90.8 LP, 90.2 HP
Turbine efficiency, %	91.8	92.2
Number compressor stages	18	8 + 8
Number turbine stages	8	9
Number of journal bearings	2	3
Generator drive end	Compressor	Compressor
Thrust bearing position	External to PCRV	External to PCRV
Inlet and exit losses, ($\Delta P/P$) %	1.80	2.85
Secondary cooling flow, %	3.6	3.8
Machine diameter, m (ft)	3.5 (11.5)	3.5 (11.5)
Machine length, m (ft)	11.3 (37)	15.8 (52)
Rotor weight, kg (tons)	60,800 (67)	68,000 (75)
Overall weight, kg (tons)	276,800 (305)	320,000 (>350)

GA-A14381

4. To simplify the recuperator-to-core return duct (i.e., no mechanical connections at top of recuperator assembly).

Both the precooler and the intercooler contain integral return tube arrangements, and although described in Section 4, they are not in the engineering stage. The complex lead tube geometries below the heat exchanger assembly, for units containing a multiplicity of modules, is of concern. The precooler is partially isolated from the turbomachine cavity, which permits the water inlet and outlet pipes to penetrate the bottom head of the PCRV. The intercooler, mounted above the turbomachine cavity, has side water inlet and outlet pipe penetrations similar to the precooler in the 3-loop nonintercooled design. This permits plugging of the modules from outside the vessel (man access not mandatory) and an inverted "U" flow arrangement, which allows drainability and rapid dumping of the intercooler water inventory. The merits of bottom supporting the helium-to-water heat exchangers are known, and the current designs incorporate this approach. Further details of the heat exchangers are given in Section 4, and Table 3-2 presents a condensed comparison of the exchangers for the two plant variants.

The size of the 2-loop intercooled plant PCRV has increased substantially, compared with the 3-loop nonintercooled reference plant. A summary of the primary system for the 2-loop intercooled plant is shown in Table 3-3. The utilization of PCRV volume is inferior to the 3-loop nonintercooled arrangement, based on the configuration selected. It is expected that this situation can be improved in future design iterations.

3.1.2 Power Conversion Loop Gas Flow Paths

Leaving the core, the gas flows in a single duct (in each loop) to the turbine. The turbine inlet duct is the only gas flow path boundary which must be mechanically retracted for machine installation and removal. After expansion in the nine-stage turbine, the gas flows up into the low-pressure side of the recuperator. After giving up its heat to the high pressure helium gas stream, the gas is transported to the precooler cavity in a

TABLE 3-2
GAS TURBINE HTGR HEAT EXCHANGER COMPARISON

Plant	3-loop Nonintercooled	2-loop[(a)] Intercooled
Recuperator		
Number per plant	3	2
Effectiveness	0.898	0.898
Tube material	Ferritic, 2-1/4 Cr-1 Mo	Ferritic, 2-1/4 Cr-1 Mo
Overall diameter, m (ft)	5.1 (16.75)	6.25 (20.5)
Overall length, m (ft)	18.9 (62.0)	22.2 (73)
Surface area/plant, m^2 (ft^2)	100,000 (1.08×10^6)	97,800 (1.05×10^6)
Overall weight, kg (tons)	430,000 (474)	680,270 (750)
Assembly location	Factory	Site
Precooler		
Tube material	Medium carbon steel	Medium carbon steel
Overall diameter, m (ft)	4.72 (15.5)	4.8 (15.8)
Overall length, m (ft)	22.3 (73)	18.3 (60)
Surface area/plant, m^2 (ft^2)	91,900 (990,000)	42,000 (452,000)
Overall weight, kg (tons)	404,000 (445)	382,000 (420)
Assembly location	Factory	Factory
Intercooler		
Overall diameter, m (ft)	No intercooler	4.4 (14.5)
Overall length, m (ft)	No intercooler	21 (69)
Surface area/plant, m^2 (ft^2)	No intercooler	32,200 (346,200)
Overall weight, kg (ton)	No intercooler	331,000 (365)
Assembly location	No intercooler	Factory

GA-A14381

[(a)] Initial conceptual design for intercooled plant.

TABLE 3-3
SUMMARY OF PRIMARY SYSTEM FOR 2-LOOP INTERCOOLED PLANT[a]

Reactor Arrangement	Reactor thermal rating, MW(t)	3000
	Plant type	Integrated
	Cycle selected	Intercooled
	Heat rejection	Dry-cooled
	Reactor outlet temperature, °C (°F)	850 (1562)
	Number of power conversion loops	2
	Loop rating	1500
PCRV	Turbomachine orientation	Chordal
	Diameter, m (ft)	39 (128)
	Height, m (ft)	38.1 (125)
	Hot duct replaceability	Yes
	Man access for bearing inspection	Yes
	Warm or cooled liners	No (could be incorporated)
	Maximum system pressure, MPa (psia)	7.93 (1150)
Turbomachine	Turbomachine type	Single shaft (60 Hz)
	Number of turbine inlet ducts	One
	Rotor construction	Welded
	Turbine Blading	Uncooled, IN-100 alloy
	Incorporation of burst shields	Yes
	Compressor/turbine stages	8 + 8/9
	Compressor pressure ratio	3.0 (1.732/1.732)
	Generator drive end	Compressor
	Overall diameter, m (ft)	3.5 (11.5)
	Overall length, m (ft)	15.8 (52)
	Assembly weight, kg (ton)	Estimated 320,000 (>350)
	Number of journal bearings	3
	Thrust bearing location	External to PCRV
	Generator type (standard)	Water-cooled stator/H_2 cooled rotor and gap
Recuperator	Type (modular construction)	Tubular, axial flow
	Number per plant	2
	Overall diameter, m (ft)	6.4 (21)
	Overall length, m (ft)	20.7 (68)
	Approximate weight, kg (ton)	680,270 (750)
	Safety classification	Nonnuclear
	Final assembly location	Site
Precooler	Number per plant	2
	Water outlet temperature, °C (°F)	86.9 (188.5)
	Overall diameter, m (ft)	4.9 (16)
	Overall length, m (ft)	22.6 (74)
	Approximate weight, kg (ton)	381,130 (420)
	Safety classification	Nonnuclear
	Final assembly location	Factory
Intercooler	Number per plant	2
	Water outlet temperature, °C (°F)	65.6 (150)
	Overall diameter, m (ft)	4.33 (14.2)
	Overall length, m (ft)	22.6 (74)
	Approximate weight, kg (ton)	331,215 (365)
	Safety classification	Nonnuclear
	Final assembly location	Factory
Performance	ISO data, °C (°F)	15 (59)
	Net electrical output, MW(e)	1237
	Station efficiency, %	41.23

[a]The 2-loop intercooled plant data are for an initial conceptual design, which lacks the design definition of the 3-loop reference plant.

short, inclined duct. After giving up its heat to the cooling water, the low-pressure helium exits from the bottom of the precooler cavity and is transported to the turbine discharge end of the turbomachine cavity. Entering the cavity, there is a transition from a circular duct to an annular geometry, with the gas flowing axially in an annulus to the vicinity of the LP compressor inlet.

After the first stage of compression ($R_c = 1.732$), the intermediate pressure gas is transported in a vertical duct to the intercooler, where in flowing upwards it gives up its heat to the cooling water. At the top of the intercooler assembly the cooled gas (i.e., returned to the original LP compressor inlet temperature) turns through 180 degree and flows back down in an annular geometry to the bottom of the intercooler cavity; then, via two short vertical ducts, the gas enters the inlet to the HP compressor. After compression to the system maximum pressure (in the second compressor unit), the gas is dumped into the center portion of the turbomachine cavity and flows into the integrally formed vertical compressor discharge duct (which in the lower plane surrounds the reactor-to-turbine duct). The high-pressure gas is directed toward the top of the recuperator assembly, where it enters the subheaders in the plane of the domed support plate. Flowing down inside the tubes (of the contiguously formed hexagonal modules) heat is regeneratively picked up from the hot turbine discharge gas. At the bottom of the modules the gas undergoes a 180 degree change in direction and is transported upward inside the integrally formed center return tubes. This heated gas flows up to the top of the recuperator assembly and is transported, via a short duct, back to the core, thus completing the flow path in the primary circuit.

3.2 PCRV DESIGN

The 2-loop intercooled plant conceptual PCRV design is shown in Figs. 3-1, 3-2, and 3-3. The PCRV diameter [39 m (128 ft)] is determined by multiplying the diameters of the three largest cavities, those of the two recuperators, and of the reactor, and the compressive stress capability of the four relevant concrete ligaments, by the maximum cavity pressure. The overall height of the PCRV is determined by the recuperator cavity height, the turbomachine cavity diameter, and the two relevant concrete ligaments between the base mat and the two cavities.

The power conversion loop (PCL) is compact, with short, straight ducts, except for the long vertical HP compressor outlet duct, which also is used as a core outlet duct service port, as has been used previously in GA GT-HTGR PCRV designs.

The PCRV (and containment) diameter would be reduced approximately 4 m (13.1 ft) if the larger diameter, high pressure upper sections of the recuperator cavities could be shortened approximately 1.83 m (6 ft). The recuperator cavities would then not exist at the same elevation as the reactor cavity, but would be only in the top head.

The PCRV (and containment) height could be reduced up to 3.05 m (10 ft) if the recuperator cavity were shortened or if it were not placed above the turbomachine cavity. The PCRV height would then be determined by the height of the reactor vessel and its two heads.

If the recuperator location was exchanged with that of the precooler cavity location, the PCRV height could be reduced, but the PCL duct lengths (and thermal barrier surface areas) would increase. It is likely that the 19° included angle between turbogenerator shafts would need to be increased, which would bring the generator ends closer together, and thus make room for the larger recuperator cavities at the opposite side of the PCRV. The reactor inlet ducts would then be close and would be on the same side of the reactor inlet plenum. Also, it is likely that one of the core auxiliary cooling system (CACS) cavities would need to be moved to the other side of the reactor cavity, and the bypass valve system ducts could become less compact.

Table 3-4 shows a comparison of primary system materials between the 3-loop nonintercooled plant and the 2-loop intercooled plant. Concrete

TABLE 3-4
COMPARISON OF PRIMARY SYSTEM MATERIALS

	2-Loop Intercooled Plant	3-Loop Nonintercooled Plant
Concrete volume (m^3)	34,142	29,435
Volume ratio	1.16	1
Precast panel ratio	1.27	1
Steel weight (tonnes)		
Core cavity liner	181	181
Refueling penetration	254	254
CACS liners	118	118
Cavity lines		
Recuperator	271	248
Precooler	221	199
Intercooler	132	0
Turbomachine	241	136
Vertical duct	100	88
PCL duct	110	140
Closures	1128	980
Bypass valve liners	50	67
Miscellaneous wells	39	39
Holddown plates	55	50
Total weight (tonnes)	2930	2470
Weight ratio	1.186	1

GA-A14381

TABLE 3-4 (Continued)

	2-Loop Intercooled Plant	3-Loop Nonintercooled Plant
Circumferential Prestressing System (CPS)		
Wire length (m)	3.10×10^6	2.05×10^6
Wire ratio	1,508	1
Diagonal tendon length (m)	4,150	4,316
Diagonal tendon ratio	0.962	1
Longitudinal Prestressing System (LPS)		
Cavity		
Number	571	552
Length (m)	35.95	33.85
Peripheral		
Number	78	72
Length (m)	29.55	31.40
T/M longitudinal		
Number	38	63
Length (m)	24.10	18.60
Summation: number times length	23,748.15	22,117.8
Weight ratio	1.0737	1
Thermal barrier		
Class A (m^2)	3,823	3,365
Class A ratio	1.136	1
Class A/B (m^2)	1,160	1,803
Class A/B ratio	0.643	1
Class B (m^2)	177	165
Class B ratio	1.072	1
Class C (m^2)	100	100
Class C ratio	1	1

volume, steel liner and penetration weights, longitudinal and circumferential prestress tendon and wire lengths, and thermal barrier surface area comparisons are made. The 2-loop intercooled plant design requires more material in all areas except for the diagonal tendons at the turbomachinery level and the Class A/B thermal barrier. The reduction in number of tendons results from the subject design having fewer, lower-pressure turbomachine cavities oriented nearly parallel to each other; however, a turbomachinery cavity liner weight penalty results from the double wall liner design. Another advantage of the 2-loop intercooled plant is the existence of a compact PCL, which contains significant quantities of cool gas because of the intercooled cycle.

A three dimensional, finite element structural analysis of the 2-loop intercooled plant has not been made, as was done for the 3-loop nonintercooled plant; however, global and local principal stress effects have been hand calculated and used in the design.

4. COMPONENT CONCEPTUAL DESIGN

4.1 HEAT EXCHANGERS

The heat exchanger design activities carried out during this report period were aimed exclusively at supporting the 2-loop intercooled plant evaluation studies. Before the initial plant layout work could proceed, it was necessary to identify preliminary envelopes for the recuperator, intercooler, and precooler in sufficient detail to permit an early assessment of their integration within the PCRV.

The envelope identification process was based on the cycle conditions summarized in Section 2. Guidelines followed in this effort were as follows:

1. Heat transfer matrix compactness was consistent with contiguous hexagonal module packaging and module designs, based on the integral return tube (IRT) approach for all designs.

2. Plain tubular surface geometries were present in all three heat exchangers (recuperator, precooler, and intercooler), with maximum tube diameter for the available envelope.

3. Bottom support was included for the precooler and intercooler.

To accomplish the first guideline, the influence of contiguous hexagonal module packaging was approximated by considering the heat exchangers to be homogeneous tube fields, with a 70% overall frontal area packing efficiency, which is consistent with previous GA designs. Since this assumption did not account for the constraints that this style of packaging tends to impose on tube pitching, minor inconsistencies between the early results and those from subsequent detailed layout work arose, but they did not influence the outcome of the intercooled plant study covered in this report.

The approach taken in these studies and the results obtained from them are discussed in the following paragraphs.

4.1.1 Preliminary Heat Exchanger Studies

4.1.1.1 Recuperator. The recuperator diameter influences the overall PCRV diameter, and its location above the turbomachine cavity (as in the 3-loop, nonintercooled plant design) creates a tight envelope on overall height. Figure 4-1 presents a family of recuperator thermal size solutions for various combinations of ITB (recuperator diameter inside cavity thermal barrier), tube pitching, and pressure loss. Since minimum-length recuperators for this type of design tend toward smaller tube diameters (i.e., $L \propto d^{1.2}$), all of the cases considered in Fig. 4-1 are based on 11.1-mm (7/16-in.) OD tubes, corresponding to the minimum practical limit adopted for GT-HTGR recuperator design. From an overall relative pressure loss standpoint, the curves are historically consistent in showing minimum inflections of approximately 1.40 pitch-to-diameter ratio (P/D). The recuperator thermal size solution selected for the initial plant layout required a 6.4 m (21 ft) ITB, 11.9 m (39 ft) effective heat transfer length, and a 1.40 p/d; its estimated pressure loss of 2% is close to the 1.93% goal indicated in the preliminary cycle conditions.

4.1.1.2 Water-Cooled Heat Exchangers (Intercooler and Precooler). From a plant layout standpoint, the intercooler length was considered to be more critical than the precooler length, because the location of the precooler above the turbomachine and its relatively lower approach temperature difference tended to create conflicting requirements on its overall height. The height problem became apparent in the initial thermal sizing surveys, which were based on a common intercooler and precooler water outlet temperature of 76.7°C (170°F), in accordance with early cycle considerations. While

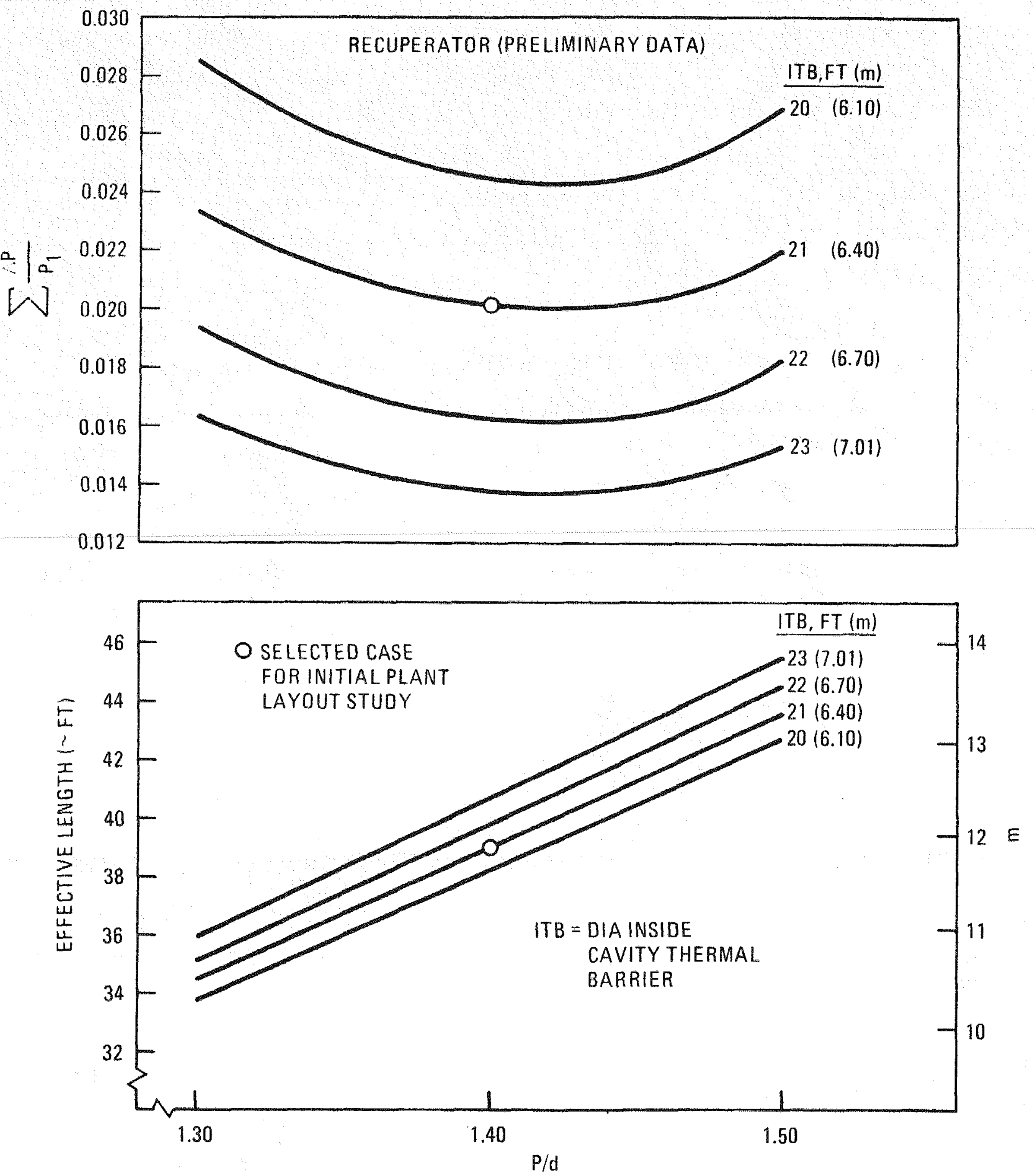

NOTES

1. TUBES ARE 7/16" OD X 0.032" WALL
   (11.1 mm OD X 0.8 mm WALL)
2. 10% UA MARGIN
3. FRONTAL AREA PACKING
   EFFICIENCY = 70% (ALL CASES)

GA-A14381

Fig. 4-1. Preliminary sizing study for recuperator 2-loop intercooled plant considerable design selection latitude existed for the precooler, acceptable intercooler solutions that did not penalize PCRV height could not be found. In addition, it was found that the usual design options to reduce length (increase shroud diameter, decrease P/D, decrease tube OD) could not be applied without forcing the Reynolds numbers in the cold end of the water circuit below 5000, where there is uncertainty in predicting heat transfer coefficient.

Length reductions available by enhancing surface geometries (e.g., finned tubing) were not investigated but were reserved as a design option if other alternatives could not be found. Unlike the 3-loop, nonintercooled GT-HTGR plant, where PCRV height considerations mandated the consideration of an internally enhanced surface geometry for the precooler, the cycle heat rejection in the 2-loop, intercooled plant was borne by the intercooler as well as the precooler. Having the cycle heat rejection borne by both the intercooler and the precooler reduced the thermal duty on the individual heat exchangers to the point where it appeared that the need for surface enhancement could be avoided.

The lack of flexibility in the design of the precooler, when examined in perspective with the intercooler length problem, suggested that the 76.7°C (170°F) common water outlet temperature requirement was not optimum. The option of varying the water outlet temperatures on these heat exchangers was considered, to find a more favorable logarithmic mean temperature difference (LMTD) balance between them, while maintaining a mixed intercooler/precooler water flow to the tower at the original 76.7°C (170°F). The influence of water outlet temperature on the effective length requirements ($L \propto \frac{1}{LMTD}$) for the precooler and intercooler is shown in Fig. 4-2, which indicates the possibility of temperature combinations that result in plain-tube design solutions, in which neither heat exchanger governs PCRV height. Although the ultimate water outlet temperature combination to be used for detailed heat exchanger design would require a separate optimization study, the initial plant layout effort required only that precooler and intercooler thermal sizes that do not influence PCRV size be identified.

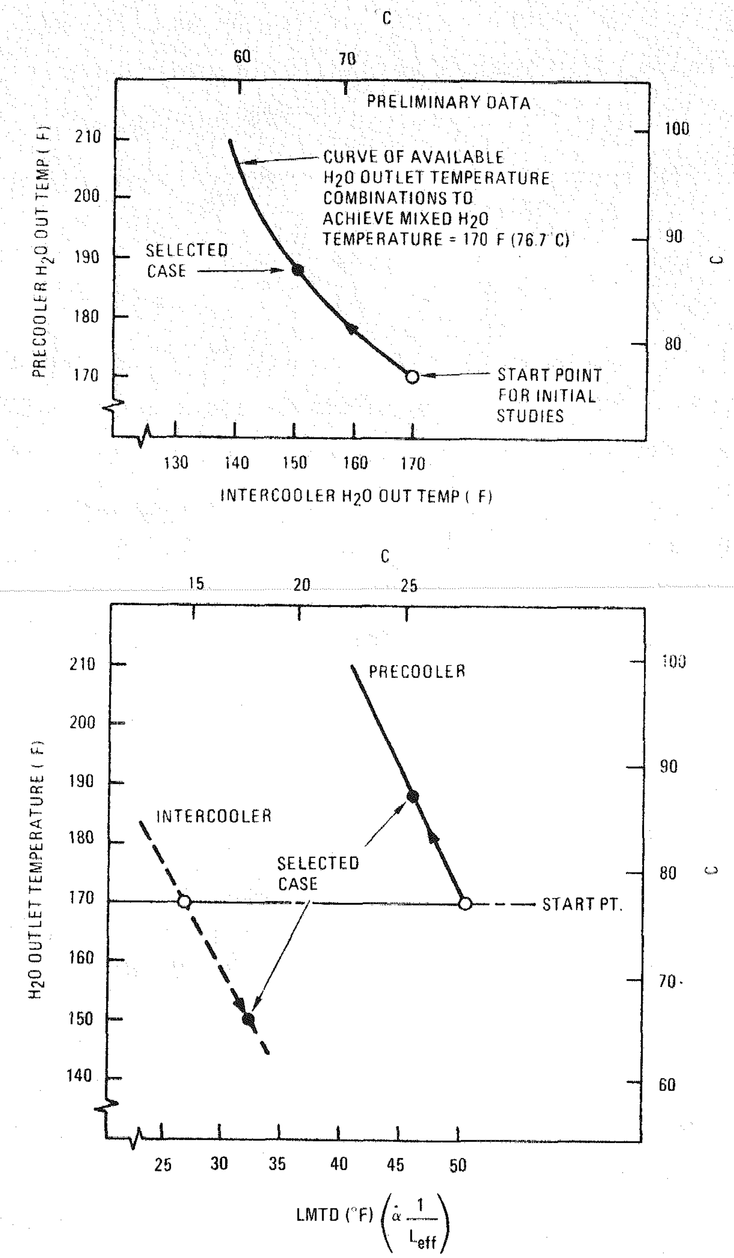

SCALING OF SELECTED CASE:

HX	L_{OLD}	X	$\frac{LMTD\ NEW}{LMTD\ OLD}$	≈	SCALED L_{NEW}	COMPUTER SOLUTION L GENSIZ	
	FT				FT	FT	(m)
INTERCOOLER	55	X	0.8	~	44	42.4	(12.9)
PRECOOLER	38	X	1.1	~	41.8	43.1	(13.1)

GA-A14381

Fig. 4-2. Procedure used for establishing precooler and intercooler thermal sizes for initial 2-loop intercooled plant layout study

This was accomplished first by scaling the effective lengths of the most acceptable 76.6°C (170°F) common water outlet temperature solutions, in accordance with the new LMTD values obtainable from noncommon water outlet temperatures shown in Fig. 4-3, then by confirming the new thermal sizes by computer analysis.

4.1.2 Follow-On Studies

Refinements to the designs previously described proceeded concurrently with the layout work, to achieve sufficient heat exchanger mechanical definition for the identification of potential problem areas. Table 4-1 summarizes the main features of the recuperator, precooler, and intercooler designs, which were designed in sufficient detail to account for the mechanical packaging of modules and the computation of primary structural gauges. Since conversion of the GA heat exchanger design codes to accommodate the heat transfer correlations to be used jointly by the GT-HTGR and HHT projects was still in process during this effort, the intercooler and precooler thermal sizes were based on the original GA correlations. On the other hand, since the near-linear fluid temperature gradients in the recuperator permitted single-node thermal sizing based on average fluid properties to be carried out with little loss of accuracy, it was possible to account for the new correlations in the recuperator by simple hand computation. The recuperator effective length stated in Table 4-1 is approximately 4.5% higher than that generated by the original GA correlations. The small differences in effective length, tube pitching, number of tubes, and heat exchanger diameter between the results in Table 4-1 and their counterpart values indicated in Fig. 4-1 and 4-2 are attributable primarily to the influence of contiguous hexagonal module packaging previously mentioned.

A conceptual layout of the recuperator is shown in Fig. 4-3. The mechanical design of this unit was given more study than that of the precooler and intercooler because its large size presented problems, from the standpoint of PCRV diameter, torispherical tubesheet forging feasibility,

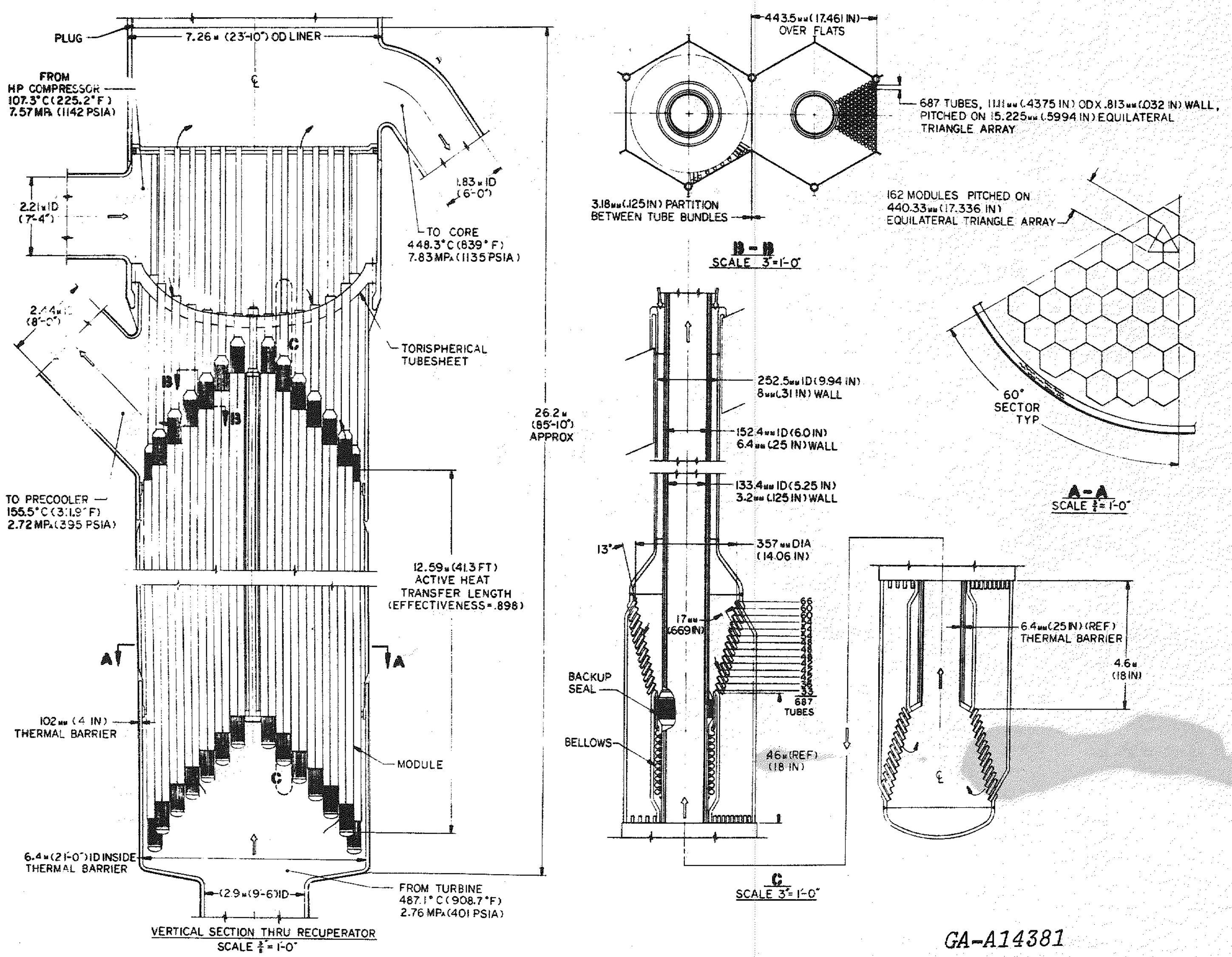

Fig. 4-3. Recuperator for 2-loop intercooled plant

TABLE 4-1
SUMMARY OF HEAT EXCHANGER CONCEPTUAL DESIGNS FOR 2-LOOP INTERCOOLED PLANT

	Exchanger	Recuperator	Precooler	Intercooler
Type	Number per plant	2	2	2
	Matrix type	Plain tubular	Plain tubular	Plain tubular
	Flow configuration	Counterflow	Counterflow	Counterflow
	Construction	Modular	Modular	Modular
Thermal	Heat transfer rate, MW(t) per reactor	2550	1011	627
	LMTD, °C (°F)	43.3 (77.89)	25.5 (45.9)	18 (32.4)
	Effectiveness	0.898	0.959	0.936
	Helium (ΔP/P)	0.020	0.014	0.010
Surface Geometry	Tube outer diameter, mm (in.)	11.1 (0.4375)	15.9 (0.625)	15.9 (0.625)
	Tube wall thickness, mm (in.)	0.8 (0.032)	1.6 (0.063)	1.6 (0.063)
	Tube pitch arrangement	Triangular	Triangular	Triangular
	Pitch/diameter ratio	1.37	1.40	1.40
	Maximum metal temperature, °C (°F)	467.2 (873)	82.2 (180)	111 (232)
	Material type	Ferritic 2-1/4 Cr-1 Mo	Medium carbon steel	Medium carbon steel
Tube Bundle Details	Hexagonal module dimension, mm (in.)	440 (17.34)	410 (16.15)	410 (16.15)
	Modules/exchanger	162	108	84
	Tubes/module	687	297	297
	Effective tube length, m (ft)	12.6 (41.3)	13.1 (43.1)	12.9 (42.4)
	Surface area/plant, m^2 (ft^2)	97,800 (1.05×10^6)	42,000 (452,000)	32,160 (346,200)
	Cavity diameter (ITB), m (ft)	6.4 (21)	5.0 (16.4)	4.7 (15.5)
Overall Assembly	Approximate overall length, m (ft)	22.2 (73)	18.3 (60)	21 (69)
	Overall diameter, m (ft)	6.25 (20.5)	4.8 (15.8)	4.4 (14.5)
	Module weight, kg (lb)	3292 (7260)	3186 (7026)	3135 (6912)
	Approximate assembly weight, tonne (tons)	680 (750)	381 (420)	331 (365)
	Assembly location	Site	Factory	Factory

and site assembly considerations. The layout shows that the tubesheet diameter is approximately 7 m (23 ft), which is the limit of U.S. vendor capabilities for one-piece forgings. The 680 tonne (750 ton) installed weight of this heat exchanger, in conjunction with its overall size, make overland transportation of this unit impractical. The design in Fig. 4-3 therefore considers final assembly operations, comprising assembly of the modules and standard pipe welds, to be accomplished at the site, with installation of the completed unit in the PCRV by means of hydraulic jacking techniques.

Additional mechanical design studies will be required to establish the final configuration and sealing approach for the cold HP helium to hot HP helium pressure boundary above the primary tubesheet of the recuperator. This area, which sees only the pressure differential developed across the HP side of the recuperator, is not viewed as a design problem at this time. The design shown in Fig. 4-3 calls for the HP return tubes to be welded to a flat tubesheet, which will be permitted to float axially within the PCRV cavity by using a circumferential sliding seal similar in design to the anti-by-pass seal employed around the periphery of the modular array. This approach permits the use of straight HP return tubes (a fabrication and maintenance advantage) and further exploits the pressure containment role of the PCRV cavity to eliminate the parasitic structure associated with an upper drum header. Considerations to be addressed later include tube-to-tube differential expansion, options for transferring the sliding seals to the tube/tubesheet interface, tradeoff incentives (if any) for a dished, rather than flat, tubesheet, and provisions for leak detection and repair.

Although conceptual layouts of the precooler and intercooler were beyond the scope of this current study, a precursory examination of the mechanical design and general feasibility aspects of these heat exchangers appeared to be warranted, particularly since the intercooler is a relatively new addition to the GT-HTGR program. A schematic of an intercooler mechanical layout is shown in Fig. 4-4. The precooler arrangement would be identical to the intercooler, except there would be no shroud, the flow

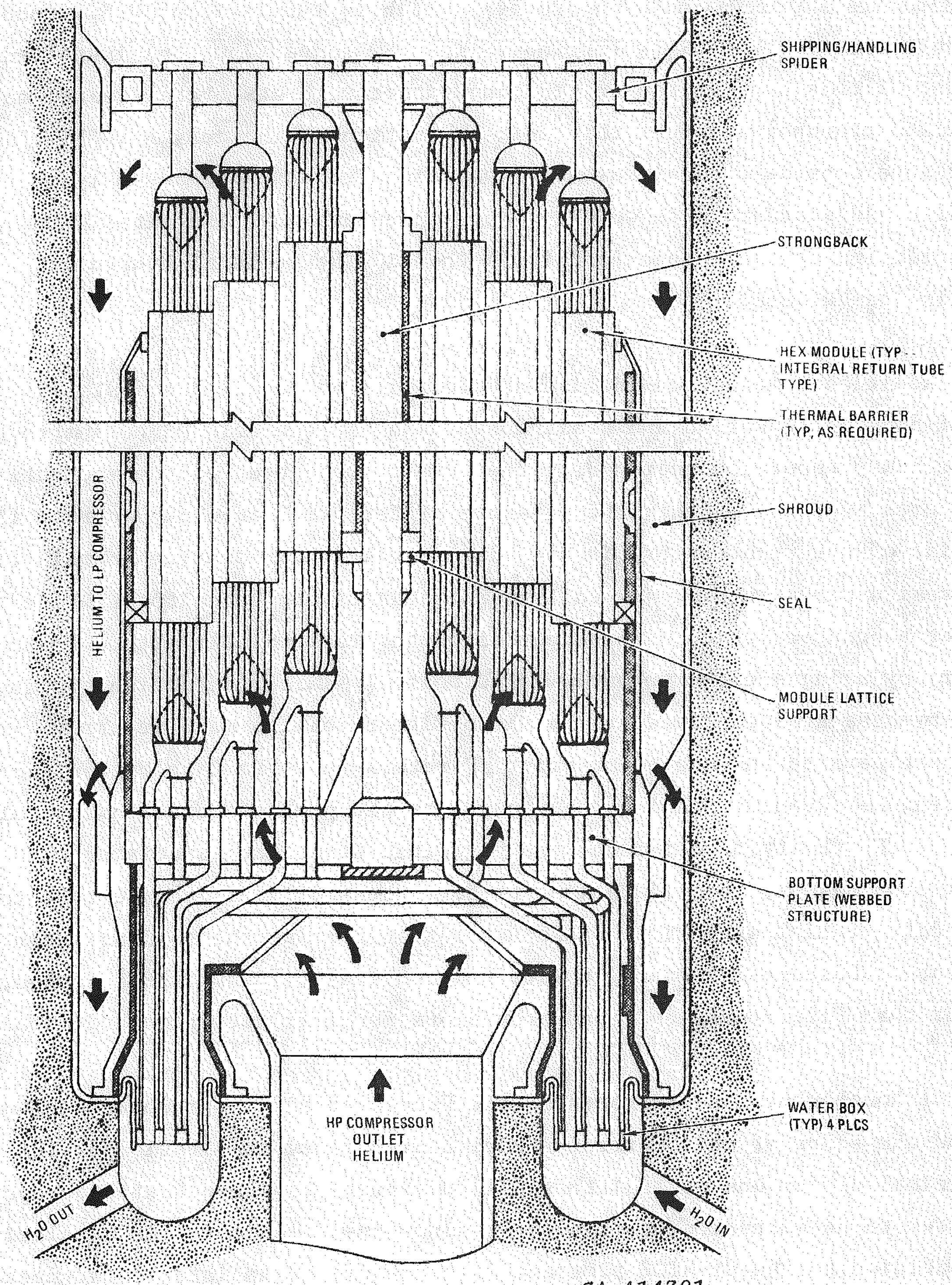

Fig. 4-4. Intercooler mechanical layout

directions would be reversed, and the plumbing below the water boxes would be routed vertically downward through the bottom head of the PCRV.

The approach used in the precooler mechanical arrangement is based upon general design principles followed for the 3-loop, nonintercooled GT-HTGR precooler, viz: 1) bottom support with upward differential thermal growth is provided in the modules, 2) contiguous hexagonal module packaging is used, 3) drainability of water passages is provided, 4) remote-control module plugging is accessible, 5) removability/reinstallation is based upon minimum man-access at the bottom of the cavity, and 6) modules and lead tubes are sized on the basis of PCRV cavity water ingress considerations (i.e., small modules and pipes relative to HHT designs).

Until more detailed design studies prove otherwise, it appears reasonable at this point to employ contiguous module packaging, even though the intercooler (and precooler) diameters probably will not control PCRV size, since there are strong incentives to keep the heat exchanger shipping diameter to a minimum and to avoid site fabrication; moreover, the hexagonal latticework of partitions separating the module tube bundles provides inherent stiffness in the overall array, for accommodating seismic and handling loads. In addition, the problem of preventing helium bypass of the tube bundle is minimized (no intermodule seals required), and heat exchanger assembly may be facilitated.

A key feature of the mechanical approach is the confinement of the subheadering water risers in the intercooler and downcomers in the precooler within their respective modules, to achieve a construction similar to that of the IRT concept applied in the recuperator. This is a conceptual alternative that will require additional structural and mechanical design study before its adoption can be recommended. It should be noted that both heat exchangers are based on the same module geometry and have similar effective lengths, which suggests an obvious opportunity for obtaining cost effectiveness through specification of a common module design for the two units. Since neither design is optimum from an overall system standpoint, additional study will be required to confirm the viability of this alternative. Other mechanical design aspects of the precooler and intercooler that will need to be addressed further include 1) evaluation of the integral return tube (IRT) module approach, wherein the water downcomer (or riser, in the case of the intercooler) circuitry is incorporated internally within each module, 2) headering of the water circuitry to satisfy requirements for minimum PCRV water ingress, remote tube plugging capability, differential thermal expansion, and compatibility with the bottom support plate, and 3) additional definition of the intercooler-to-HP compressor helium flow circuitry.

4.2 TURBOMACHINE

The Power Systems Division of United Technologies Corporation, supported by the Pratt and Whitney Group/Commercial Products Division, has undertaken the conceptual design of two closed-cycle helium gas turbines of approximately 1500 MW(t) power input. These turbomachines represent a 50% increase in power from the 1000 MW(t) design studied in FY 1976. One of these new designs incorporates an intercooler midway through the compression process and has increased compressor pressure ratio. The other design is a scale-up of the previously studied 1000 MW(t) design. The time and effort allotted for these conceptual design studies was substantially less than was expended on the 1000 MW(t) design, as it was necessary to concentrate only on those items having a major impact on performance and structural configuration. The results of these studies should be recognized as initial efforts, without benefit of cost performance optimization. However, they are indicative of the level of performance, size, and general appearance that the turbomachine would have, with the constraints imposed by the PCRV requirements.

A discussion of the intercooled and nonintercooled designs, as they are defined in the conceptual design study, is presented in the following paragraphs. For the new intercooled machine, the helium man-flow rate, pressure ratio, and turbine inlet temperature were defined by GA, as described in Section 2 of this report. As in previous studies, a constraint of 3.5 m (11.5 ft) was put on the turbomachine diameter, to facilitate rail transportation when the contaminated machine assembly is installed in a shielded cask.

4.2.1 Intercooled Turbomachine Conceptual Design Study

4.2.1.1 Compressor Design. At the beginning of the study, the effects of compressor pressure ratio split and overall pressure ratio were evaluated to assist in selection of the compressor designs. This study showed that splitting the compressor pressure ratio evenly was nearly optimum, as was the overall pressure ratio of 3.0 specified by GA.

The 1500 MW(t) intercooled cycle requires two compressors with a combined pressure ratio of 3.0. The following three compression systems were investigated for use in this cycle:

1. An 8-stage low-pressure compressor (LPC) and an 8-stage high-pressure compressor (HPC) with a common flow path inside diameter of 1854 mm (73 in.). The pressure ratio for each compressor was 1.73.

2. A 10-stage LPC and an 8-stage HPC with a common flow path inside diameter of 1676 mm (66 in.). The pressure ratio was split 1.84 on the LPC and 1.62 on the HPC.

3. A 10-stage LPC and a 10-stage HPC with a common flow path inside diameter of 1549 mm (61 in.). The pressure ratio was evenly split at 1.73 for each compressor.

Tables 4-2 and 4-3 present detailed comparisons of these compressors. Overall cycle estudies determined that an even pressure ratio split was optimum from an overall thermal efficiency standpoint. This eliminated configuration 2, since its pressure ratio split reduced thermal efficiency 0.3 points. Configuration 1 [8 & 8 at 1854 mm (73 in.)] was selected for the intercooled cycle because of its shorter length relative to configuration 3. It should also be noted that an even number of stages was maintained for these compressors, to preserve the concept of carrying two blade rows per disk.

TABLE 4-2
LOW-PRESSURE COMPRESSOR DESIGNS

	Selected Design	Alternate	Designs
No. of Stages	8	10	10
PR	1.732	1.845	1.732
ηAD/poly	0.908/0.917	0.912/0.922	0.916/0.925
Surge margin	9.5%	9.5%	9.5%
ID (construction), mm (in.)	1854 (73)	1676 (66)	1549 (61)
Maximum OD, mm (in.)	2182 (85.92)	2034 (80.06)	1930 (75.99)
$W\sqrt{\theta_2}/\delta T_2$	63.39	63.39	63.39
Aspect ratio	1.6	1.6	1.6
Gap/chord	1.00	0.955	1.00
Tip clearance	0.0120	0.0120	0.0120
Cx/U	0.464	0.510	0.544
Df	0.526	0.516	0.507
Reaction	0.75	0.75	0.75
Exit hub/tip radius	0.883	0.866	0.844
No. of blades and vanes	1364	1481	1250
Length[a], mm (in.)	1487 (58.54)	2004 (78.91)	2180 (85.84)

[a] With IGV.

GA-A14381

TABLE 4-3
HIGH-PRESSURE COMPRESSOR DESIGNS

	Selected Design	Alternate	Designs
No. of Stages	8	8	10
PR	1.732	1.626	1.732
ηAD/poly	0.902/0.911	0.905/0.914	0.906/0.916
Surge margin	10%	10%	10%
ID (construction), mm (in.)	1854 (73)	1676 (66)	1549 (61)
Maximum OD, mm (in.)	2053 (80.82)	1881 (74.04)	1782 (70.16)
$W\sqrt{\theta}/\delta T_2$	37.22	34.86	37.22
Aspect ratio	1.6	1.6	1.6
Gap/chord	0.971	0.914	0.887
Tip clearance	0.0120	0.0120	0.0120
Cx/U	0.503	0.556	0.596
Df	0.516	0.489	0.479
Reaction	0.75	0.75	0.75
Exit hub/tip radius	0.926	0.914	0.899
No. of blades and vanes[a]	2105	1940	2058
Length[a], mm (in.)	1044 (41.10)	1098 (43.24)	1500 (59.04)

GA-A14381

[a]With IGV.

4.2.1.2 Turbine Design. The turbine selected for the intercooled cycle is a nine-stage design which has a 280,000 hour creep life at an inlet temperature of 850°C (1560°F). The first eight stages of the flow path are essentially the same as those proposed for a 1300 MW(t) design studied in FY 1976. A ninth stage was added to maintain efficiency.

A comparison of the aerodynamic parameters of the 1500 MW(t) intercooled cycle and the 1300 MW(t) nonintercooled cycle is contained in Table 4-4. Due to the lower velocity ratio and Cx/U in the nine-stage 1500 MW(t) design, the foil turnings and mach numbers are higher than in the 1330 MW(t) turbine, but they are still within the acceptable design range. The expected efficiency of the nine-stage 1500 MW(t) intercooled cycle turbine is 92.2%.

Details of the selected compressors and turbine for the intercooled machine, together with the main features of the rotating machinery, are summarized in Table 4-5.

4.2.1.3 Turbine Rim Cooling Definition. Turbine disk rim and turbine case cooling has been estimated for the intercooled cycle turbine described previously. In estimating this coolant flow the following four factors were found to affect the absolute flow required: a) turbine pressure ratio, b) absolute pressure of the coolant, c) absolute temperature of the coolant, and d) total number of stages to be cooled. All of these factors changed relative to the 1330 MW(t) design, in ways that increased the coolant flow required. The mass flow through the compressor and turbine was less for the 1330 MW(t) design than for the 1500 MW(t) design; therefore, the percent of compressor flow diverted to turbine rim and case cooling increased substantially, as shown below:

	1330 MW(t)	1500 MW(t) Intercooled
Rotor coolant (% compressor flow)	2.1	3.1
Case coolant (% compressor flow)	0.6	0.7
Total	2.7	3.8

TABLE 4-4
TURBINE AERODYNAMIC PARAMETERS

Cycle	1330 MW(t) Nonintercooled	1500 MW(t) Intercooled
No. of stages	8	9
Mean velocity ratio	0.596	0.580
Cx/U	0.564	0.533
Average foil turning, degrees	84.2	80.7
Average foil mach number	0.266	0.277
Exit swirl, degrees	9.2	15.0
Exit mach number	0.107	0.111
Reaction	0.55	0.55/0.45
No. of blades and vanes	904	939
Estimated efficiency	0.924	0.922

GA-A14381

TABLE 4-5
DETAILS OF 1500 MW(t) INTERCOOLED 60-Hz TURBOMACHINE

Rotating Unit	Compressor		Turbine
	Low Pressure	High Pressure	
No. of stages	8	8	9
Hub diameter, mm (in.)			
First stage	1854 (73.0)	1854 (73.0)	1702 (67.0)
Last stage	1854 (73.0)	1854 (73.0)	1613 (63.5)
Tip diameter, mm (in.)			
First stage	2182 (85.92)	2053 (80.82)	2032 (80.0)
Last stage	2100 (82.67)	2002 (78.83)	2400 (94.5)
Hub/tip ratio first/last stage	0.850/0.883	0.903/0.926	0.838/0.672
Bladed length, mm (in.)	1487 (58.54)	1044 (41.1)	2591 (102)
Blading efficiency, %			
Adiabatic	0.908	0.902	0.922
Polytropic	0.917	0.911	0.906
Degree of reaction, %	75	75	55/45
Turbine secondary flow, %	--	--	3.80
Overall machine length, m (ft)	15.85 (52.0)		
Machine outer diameter, m (ft)	3.5 (11.5) Design constraint		
Rotor weight, kg (ton)	68,060 (75)		
Total machine weight, kg (ton)	To be determined		
Type of rotor construction	Welded		Welded
Blading details	--		Uncooled
Turbine blade material	--		IN 100
Blading life, hr	280,000		280,000
Rotor burst shield	Integral part of machine structure		
Journal bearing man-access	For inspection and limited maintenance[a]		
Generator drive end	Compressor end of machine		
Bearing details			
Number of journal bearings	3		
Type of journal bearings	Tilting pad, oil lubricated		
Thrust bearing type	Tilting pad, double acting		
Thrust bearing location	External to PCRV		

[a] Access means to center journal bearing not yet resolved.

GA-A14381

The turbine case cooling increased, due to the increased case length and surface area.

4.2.1.4 Critical Speed Analysis. A critical speed analysis is being performed on the 1500 MW(t) intercooled engine to determine the feasibility of a split compressor and increased overall rotor length. The analysis model is an extension of that used in the previous HTGR turbomachine studies, with allowances made to accommodate a possible third gas-generator bearing between the low- and high-pressure compressors. The rotor and case geometries have been updated to reflect the 1500 MW(t) weights and dimensions. An attempt is also being made to include the influence of the larger generator required by the increased power output. The larger 8.53 m (28 ft) output shaft has been modelled and provisions made to study the effect of adding a bearing at shaft mid span. This model should predict all rotor, case, and shaft modes of concern and will output frequencies and mode shapes at each critical speed.

The initial results of this analysis have shown that from the critical speed standpoint the 1500 MW(t) turbomachine is satisfactory, with the first free-free mode occurring at a speed of 5600 rpm, compared with 5000 rpm in the 1000 MW(t) reference design.

4.2.1.5 Rotor Weight Estimate. The following rotor weights and polar moments of inertia have been estimated for the 1500 MW(t) intercooled gas turbine design:

	Weight (∿lb)	IP (∿lb in sec^2)
Turbine rotor	48,183	82,650
Compressor turbine shafting	40,657	47,189
Compressor rotor	43,755	84,325
Output shafting (to thrust bearing)	17,388	3,643
Total rotor	149,983	217,807

The following 1-g bearing reactions were calculated for these rotor weights:

No. 1 Bearing (turbine end)	52,155 lb
No. 2 Bearing (compressor center)	59,922 lb
No. 3 Bearing (compressor end)	26,292 lb
No. 4 Bearing (thrust)	11,614 lb

These rotor weights are consistent with the blade attachment design, disk spacer, and disk thickness, as shown on the engine cross section (Fig. 4-5). The compressor weights were estimated using a combination of digitized rapid analysis of weights (DRAW) program, the weight engineering rub comp code, and the disk programs.

The rub comp program defines the weight distribution of the disks, stage by stage, and the design disk program defines the actual disk weight for the 5th and 6th disk. The DRAW program verified the weights from the layout and calculated polar moment of inertia. The disk weights were based on an average tangential stress of 76,000 psi and a radial stress level of 100,000 psi. The turbine weights were estimated in a similar manner, using the rub turbine and DRAW programs, and the same stress levels as used in the compressor. The shaft weights and polar moments of inertia were derived, using the engine cross section drawing (Fig. 4-5) and the DRAW program.

4.2.1.6 Engine Cross Section Layout and Installation Drawings. A cross section layout (Fig. 4-5) and an installation drawing (Fig. 4-6) have been prepared for the 1500 MW(t) intercooled turbomachine. The basic approach to defining the turbomachine was to adapt the design of the 1000 MW(t) nonintercooled gas turbine wherever possible. Because the 1000 MW(t) design had the benefit of a detailed mechanical and structural design effort, it appeared to be a logical starting point for the design of the 1500 MW(t) turbomachine. Basic physical constraints imposed by GA on the 1500 MW(t) design were 1) the maximum turbomachine diameter must not exceed 3.5 m (11.5 ft) and 2) only a single turbine inlet supply pipe was to be

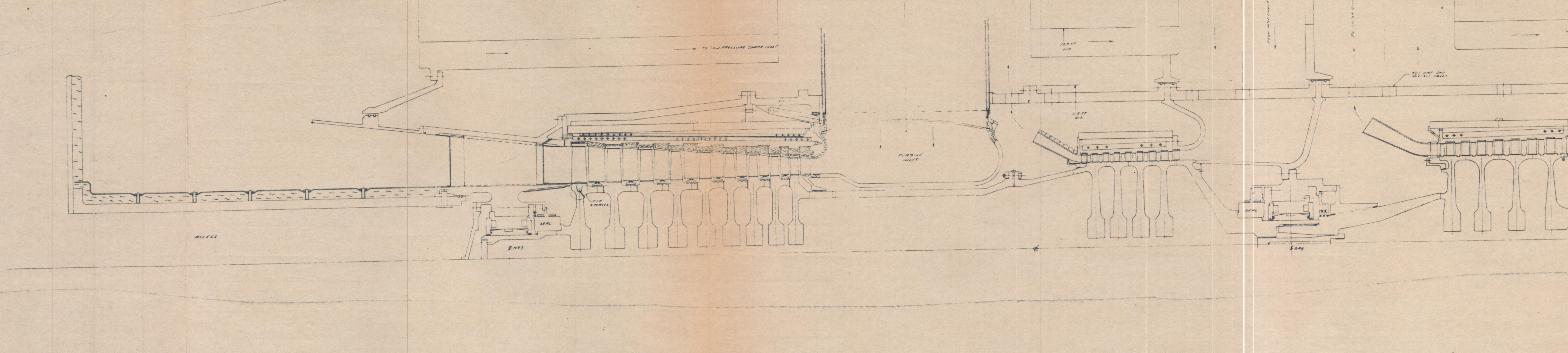

GA-A14381

Fig. 4-5. Cross section of 1500 MW(t) intercooled turbomachine

GA-A14381

Fig. 4-6. Installation of 1500 MW(t) intercooled turbomachine used. The cold or compressor-end drive to the electric generator was maintained as in previous designs because it did not require excessive thermal protection, it permitted ready access to the thrust bearing, and it minimized rotor shift, due to thermal growth. The power output shaft has been increased in diameter, consistent with increased short circuit torque. This, in turn, necessitates an increase in the size of the floating ring shaft seals in the secondary containment and PCRV plug. The shaft journal bearings have been increased to 508 mm (20 in.) at the turbine and between the compressors. The low-pressure compressor inlet-end bearing, the journal bearing at the thrust bearing, and the steady bearing (if required) for the power output shaft will all be 406 mm (16 in.) in diameter. The bearing selections are discussed further in Section 4.2.1.7.

The compressors are both eight-stage designs, in which each disk carries two of the compressor blade rows. The low-pressure compresor can be removed from the turbomachine by removing the outer case bolts and the shaft nut under the 508 mm (20 in.) bearing (through the LPC bore); the rotor radial position should be stabilized by inserting the radial bolts through the outer case. The outer case at the LPC inlet is cylindrical to provide a stiff path to ground for the load from the 508 m (20 in.) bearing between the compressors. A direct path to ground located at this bearing was considered, but it was rejected because of the uncertainty of the loading, due to the adjacent LPC inlet mount and PCRV motions.

The low-pressure compressor discharge passes through holes in the outer case similar to those at its inlet. The LPC exit cavity is sealed from the bearing, located between the LPC and HPC, with a buffered linear labyrinth seal, to permit separation from the HPC without disassembly of the seal. The seal surface is sloped, to prevent damage to the knife edges during removal or reinstallation of the LPC.

The HPC design is very similar to the reference 1000 MW(t) design. Flow enters through holes in the cylindrical case and leaves in the same manner. The turbine inlet duct supply pipe diameter has been increased from that in the 1000 MW(t) design, by a redesign of the scroll mating surface. No further increase is possible without relaxation of the 3.5 m (11.5 ft) diameter limit of the turbomachine. The increased pipe size permits the higher flow rate to be handled with almost the same losses as the 1000 MW(t) design, but the turbine supply scroll is no larger in toroidal cross section than that of the 1000 MW(t) design. This results in increased scroll losses. The higher temperature gradient across the scroll walls makes the insulated scroll more important in the 1500 MW(t) design than in the 1000 MW(t) variant design.

The 1500 MW(t) turbomachine is longer than the 1000 MW(t) reference design, due to the need for nine stages, and the case and containment have been redesigned to accommodate the extra length. The construction of the rotor is still welded disks with one blade row (tangentially attached) per disk. The exhaust diffuser and dump area are enlarged in proportion to the larger passage height, to minimize the exit losses. The turbine end of the turbomachine employs the same mount system, pin-in-clevis, as did the reference design. No solution to the access problem of the midcompressor bearing has been found, but the limited time for this task permitted only a superficial investigation of the problem.

4.2.1.7 Bearing Definition. Bearing characteristics have been defined for all journal bearings in the system and for the thrust bearing. The bearing numbering convention for the journal bearings, starting with No. 1 at the turbine end and progressing to No. 7 at the generator exciter end is similar to that used in previous designs. Note that the No. 2 bearing is now located between the LPC and HPC. (Bearing characteristics are presented in Table 4-6.) The requirement for a journal bearing on the power output shaft between the thrust bearing and the electric generator has not been established; therefore, an additional set of data for the No. 4 and No. 6 bearings is presented for the case where a No. 5 journal bearing is not used.

The 1500 MW(t) turbomachine bearing power losses have increased about 100% over those in the reference 1000 MW(t) design. There are two more bearings to service, and ancillary requirements are increased.

TABLE 4-6
JOURNAL BEARING CHARACTERISTICS, INTERCOOLED DESIGN

Bearing No.	Load W (lb)	Length x Diam LxD (in. x in.)	Unit Load W/LD (psi)	Min Pivotal Film h min (mils)	Stiffness Kxx (lb/in. x 10^{-6})	Coefficients Kyy (lb/in. x 10^{-6})	Damping Coefficients WBxx (lb/in. x 10^{-6})	WByy	Power Loss HP (hp)	Flow Q (gpm)
1	52,155	16 x 20	163	10.7	7.4	5.7	9.8	8.1	790	320
2	59,922	16 x 20	187	10.0	8.6	6.3	11.0	8.7	795	320
3	26,292	8 x 16	205	5.7	6.5	3.8	5.9	3.7	205	80
4	16,000	8 x 16	125	7.3	3.3	2.1	3.5	2.5	196	80
5	8,000	5 x 16	100	6.1	2.0	1.1	1.7	1.1	128	55
6	60,000	16 x 20	188	10.0	8.6	6.3	11.0	8.7	795	320
7	75,000	16 x 20	234	9.0	11.2	7.6	13.3	9.9	805	325
Without Bearing No. 5, data for Bearing No. 4 and No. 6 are as follows:										
4	20,000	8 x 16	156	6.4	4.5	2.5	5.1	3.5	186	75
6	64,000	16 x 20	200	9.8	9.2	6.6	11.6	9.0	795	320

The thrust bearing ID has been increased in the 1500 MW(t) design 432 mm (17 in.), to accommodate the increased output shaft diameter. In addition, hydraulic jacking will be required for a hot start when the internal pressure is about 6.89 MPa (1000 psi). The bearing OD is still 762 mm (30 in.), and eight thrust pads are still used, but further study might indicate an increase in the number of thrust pads is desirable. The design load is still 90,744 Kg (200,000 lb). The floating ring seal diameter has been increased to accommodate the larger diameter output shaft, which implies an increase in risk for the design until testing is satisfactorily completed.

4.2.1.8 Electric Generator Selection. A 720-MVA generator has been selected for both the 1500 MW(t) intercooler and the 1500 MW(t) nonintercooled designs. The expected efficiency is 98.7%, and the design is a water-cooled stator and hydrogen-cooled rotor and gap. The length, width, and height of the generator envelope (without ancillaries) are 14.2 m (560 in.), 4.57 m (180 in.), and 5.33 m (210 in.), respectively.

4.2.2 Nonintercooled Turbomachine Conceptual Design Study

4.2.2.1 Compressor Design. The 1500 MW(t) compressor is very similar to the 1330 MW(t) compressor studied previously. The only change is an increase in the outer diameter to pass the higher flow. Table 4-7 presents a detailed comparison of the 1500 MW(t) compressor in relation to the 1000 MW(t) and the 1330 MW(t) compressors.

4.2.2.2 Turbine Design. In relation to the 1550 MW(t) intercooled cycle, the 1500 MW(t) nonintercooled cycle has a 16% higher turbine inlet corrected flow, the same exit corrected flow, and a 14% lower work requirement. Several different flow paths were studied for the nonintercooled cycle. The aerodynamic parameters corresponding to these flow paths are tabulated in Table 4-8 and compared to those of the intercooled cycle turbine. The first nonintercooled cycle flow path is a nine-stage design similar to the intercooled cycle turbine flow path. The second flow path is the same nine-stage

TABLE 4-7
NONINTERCOOLED COMPRESSOR COMPARISON

	1000 MW(t)	1330 MW(t)	1500 MW(t)
No. of stages	18	16	16
$W\sqrt{\theta T_2}/\delta T_2$	40.93	55.95	61.21
Pr	2.5	2.5	2.5
ηAD/poly	0.897/0.912	0.902/0.917	0.904/0.918
Surge margin	12.5%	9.5%	10.5%
ID, mm (in.)	1575 (62)	1676 (66)	1676 (66)
Maximum OD, mm (in.)	1826 (71.90)	1995 (78.53)	2022 (79.61)
Cx/U	0.569	0.528	0.525
Aspect ratio	1.60	1.6	1.6
GAP/chord	0.8867	0.8867	0.8867
Tip clearance/span	0.0120	0.0120	0.0120
Reaction	0.75	0.75	0.75
Df	0.487	0.500	0.497
Exit hub/tip radius	0.911	0.896	0.887
No. of blades and vanes	3630	2704	2567
Length[(a)], mm (in.)	2604 (102.5)	2733 (107.6)	2913 (114.7)

[(a)] Includes IGV.

GA-A14381

TABLE 4-8
TURBINE AERODYNAMIC PARAMETERS

Parameters	1500 MW(t) Intercooled	Candidate Nonintercooled 1500 MW(t)		
First blade P/A stress, ksi	14.7	14.7	14.7	16.7
No. of stages	9	9	8	8
Mean velocity ratio	0.580	0.625	0.586	0.623
Cx/U	0.533	0.589	0.624	0.531
Average foil turning, degree	90.7	76.0	82.6	79.9
Average foil mach number	0.277	0.259	0.277	0.252
Exit swirl, degree	15.0	3.6	9.9	5.3
Exit mach number	0.111	0.100	0.121	0.098
Efficiency, %	92.2	92.6	92.2	92.6
Reaction	0.55/0.45	0.55/0.45	0.55/0.45	0.55/0.45
No. of blades and vanes	939	995	953	794
Status	--	Rejected	Chosen	Rejected

GA-A14381

flow path, but with the last stage removed. The third flow path is the 9-stage flow path with the first stage removed. The second flow path was chosen, although the first and third flow paths offered an efficiency increase of 0.4 percent. The first flow path was rejected because of the length and weight increase due to the additional stage. The third flow path was not used because of the 14% increase in the first blade stress. Since the intercooled cycle first blade is already at the maximum allowable stress to maintain the 280,000 hours life uncooled, any increase in stress would require either cooling the foil or reducing the creep life.

4.2.2.3 Turbine Stress Review. The intercooled cycle turbine design was determined to have the maximum first blade stress allowance and still be capable of 280,000 hours operation. The turbines examined for the 1500 MW(t) nonintercooled design were required to pass a higher corrected flow and required an increase in turbine annulus area or number of stages to maximize efficiency. However, the increased annulus would also mean increased blade stress and reduced creep life (to perhaps only 17 years instead of 40). The addition of an extra stage would eliminate the need for increased annulus area and thus preserve the 40-year creep life, but it would increase rotor length and weight and would probably result in unacceptable rotor critical speed margin. Therefore, the design selected was the eight-stage design with the same flow path as the first eight stages of the intercooled cycle turbine.

4.2.2.4 Turbomachine Installation Layout. An installation drawing for the nonintercooled helium gas turbine design is shown in Fig. 4-7. The basic design approach has been to scale up the 1000 MW(t) and 1330 MW(t) designs previously studied, since the compressor pressure ratio and turbine inlet temperatures are unchanged from the earlier designs. The design preserves the two-bearing simply supported rotor concept, and the outer case (or engine backbone) is similar in appearance to that of the 1000 MW(t) and 1330 MW(t) designs. The one major departure from the scale-up design approach is in the turbine inlet scroll. Due to the 3.5 m (11.5 ft)

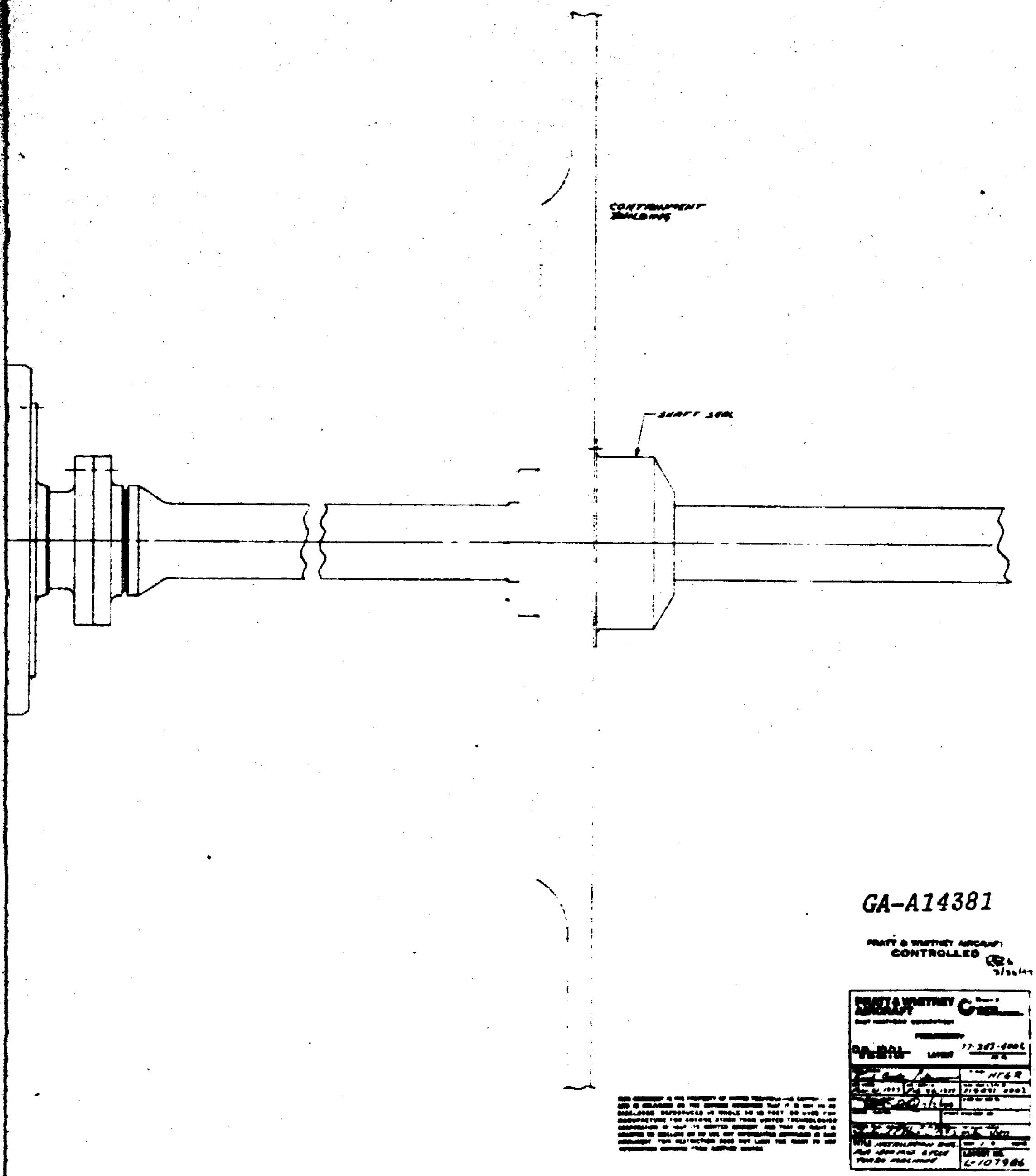

Fig. 4-7. Installation of 1500 MW(t) Nonintercooled turbomachine

maximum engine diameter limit imposed by shipping considerations, the turbine inlet scroll has not been scaled up in cross section or diameter, which results in increased pressure losses.

4.3 PRIMARY SYSTEM PRESSURE LOSS

The sensitivity of the performance of a nuclear gas turbine to system pressure losses is well known, and in previous plant designs (particularly the 3-loop nonintercooled plant) considerable effort was expended to minimize parasitic pressure losses. With the introduction of an intercooler into the primary system (and the attendant flow path geometry complexity) pressure loss minimization is of even greater importance, since excessive pressure loss tends to negate the advantage of intercooling. Accordingly, a pressure loss study was completed for the intercooled plant primary system duct losses.

At the beginning of the performance study it was thought that the overall system pressure loss would increase by about 3.0 percentage points on ($\Delta P/P$) in the following areas: 1) intercooler 1%, 2) additional duct losses 1%, and 3) additional turbomachine inlet and exit losses 1%. These assumptions proved to be essentially accurate for the primary system selected, as summarized in the following paragraphs.

4.3.1 Turbomachine Inlet and Exit Losses

It was realized that with a combination of 1) constrained machine diameter at 3.5 m (11.5 ft), 2) higher helium mass flow, and 3) additional compressor, the inlet and exit losses would be higher for the 620 MW(e) turbomachine than for the nonintercooled 400 MW(e) machine. A summary of the UTC computed losses for the turbomachine is shown in Table 4-9. The increased loss associated with an additional compressor is 0.92 percentage points. Because of the annular gas flow in the turbomachine cavity, the machine casing is perforated (for gas flow introduction) at the LP compressor inlet, which represents an additional small loss not present in the

TABLE 4-9
COMPARISON OF TURBOMACHINERY INLET AND OUTLET PRESSURE LOSSES

Plant	3-Loop Reference Nonintercooled	2-Loop Intercooled	Comments
Machine rating, MW(e)	400	Approximately 650	
Number of turbine inlets	One	One	
Machine diameter, m (ft)	3.5 (11.5)	3.5 (11.5)	Design constraint
Machine length, m (ft)	11.3 (37)	15.8 (52)	Additional journal bearing (3) required for intercooled machine
Loss data reference	UTC Report PSD-R-106 September 1976	UTC Letter AC/4351/77-7073 February 18, 1977	
Compressor ($\Delta P/P$)			
Inlet volute	0.25	0.28 LP	Includes additional casing holes
		0.23 HP	New loss
Exit diffuser	0.47	0.77 LP	Diff + dump + case holes
Diffuser dump	0.23	0.69 HP	New loss
Shell holes	0.03		
	Σexit = 0.73		
Turbine ($\Delta P/P$)			
Inlet volute	0.364	0.48	Higher because of constrained diameter for much larger machine with one inlet
Exit case struts	0.04	0.40	Summation of exit losses, reduced slightly because of larger exit flow area
Exhaust diffuser	0.09		
Exit dump	0.32		
Exit contraction	0.01		
	Σexit = 0.46		
$\Sigma(\Delta P/P)$, %[a]	1.804	2.85	Higher by the amount approximately equal to the addition of a second compressor unit

[a] Losses not strictly additive in cycle calculations but shown here to illustrate differences associated with machine design.

nonintercooled machine. Because of the increased mass flow rate and the limited flow area for the turbine inlet volute (with the constrained machine diameter), the loss in this region is higher than for the reference design. Because of the larger machine cavity diameter, there is a slight reduction in turbine exit loss. The inlet and exit losses for the 2-loop intercooled and 3-loop nonintercooled plants are 2.85% and 1.804%, respectively. With additional work and relaxation of the design constraints, it is felt that the intercooled machine inlet and outlet losses could be reduced.

4.3.2 Primary System Duct Losses

An estimate was made of the primary system duct losses, similar to that performed for the reference plant. The stations in the pressure loss analysis are identified in Fig. 4-8. The sources of the losses, together with pertinent local geometries and fluid properties, are given in Table 4-10. The actual losses, and summation of losses are given in Table 4-11. The initial run of this simplistic code showed regions of high pressure loss that required additional design. The initial run for the primary system layout (shown in Figs. 3-1, 3-2, and 3-3) revealed a sum pressure loss [$\Sigma(\Delta P/P)$, a convenient parameter but not precisely additive in the system] of 3.7% in the ducts. This was considered excessive, and an investigation of the results showed high losses associated with flow in the ducts to and from the intercooler. The following changes were recommended, but as yet have not been incorporated into the layout:

1. Increase the diameter of the HP compressor-to-intercooler duct from 1.52 m (5 ft) to 1.83 m (6 ft).

2. Increase the outside diameter of the intercooler annulus from 4.72 m (15.5 ft) to 4.87 m (16.0 ft).

2. Modify geometry of intercooler annulus outlet and exit plenum (diffuser or guide vanes).

4. Modify radius of curvature of the precooler-to-LP compressor duct.

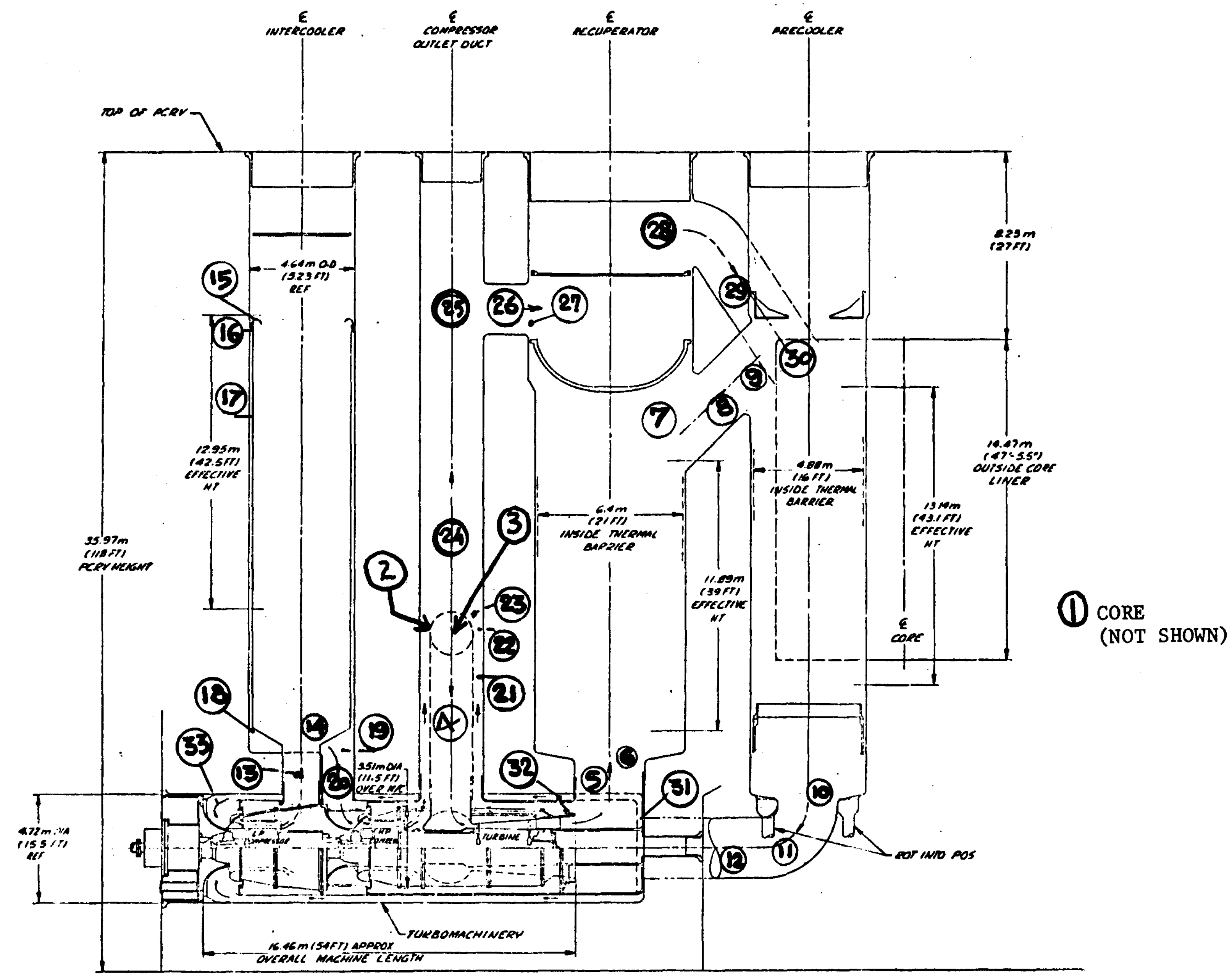

Fig. 4-8. Primary system stations used in pressure loss study

TABLE 4-10
INPUT DATA FOR INTERCOOLED PLANT PRIMARY SYSTEM PRESSURE LOSS ESTIMATE

Item	Description (See Fig. 4-8 for Locations)	L (ft)	D (ft)	A (sq ft)	K	T (°F)	P (psia)	W (10^6 lb/hr)	Misc. (lb/ft hr)
1	Core	0.00	0.00	0.00	0.000	1562	1124	5.70	0.119
2	Contraction	0.00	5.70	0.00	0.025	1562	1124	5.70	0.119
3	90 degree bend	0.00	5.70	0.00	0.510	1562	1124	5.70	0.119
4	Friction	40.64	5.70	0.00	0.000	1562	1124	5.70	0.119
5	Friction	6.00	9.50	0.00	0.000	909	405	5.90	0.091
6	Expansion	0.00	9.50	0.00	3.000	909	403	5.90	0.091
7	Wye	0.00	8.00	0.00	0.580	315	395	5.90	0.062
8	Friction	11.73	8.00	0.00	0.000	315	395	5.90	0.062
9	Expansion	0.00	8.00	0.00	1.000	315	395	5.90	0.062
10	Contraction	0.00	8.00	0.00	0.335	80	389	5.90	0.048
11	90 degree bend	0.00	8.00	0.00	1.670	80	389	5.90	0.048
12	Friction	21.30	8.00	0.00	0.000	80	389	5.90	0.048
13	Friction	6.00	6.00	0.00	0.000	225	672	5.90	0.057
14	Expansion	0.00	6.00	0.00	3.000	225	669	5.90	0.057
15	180 degree turn	0.00	1.58	37.84	0.589	79	665	5.90	0.048
16	Contraction	0.00	1.58	37.84	0.500	79	665	5.90	0.048
17	Friction	58.60	1.58	37.84	0.500	79	665	5.90	0.048
18	Expansion	0.00	1.58	37.84	0.450	79	665	5.90	0.048
19	Contraction	0.00	3.50	0.00	0.500	79	665	2.95	0.048
20	Friction	6.00	3.50	0.00	0.000	79	665	2.95	0.048
21	Annulus friction	0.00	2.50	30.43	0.122	225	1150	5.71	0.057
22	Blockage	0.00	2.50	24.00	0.010	225	1150	5.71	0.057
23	Expansion	0.00	2.50	24.00	2.150	225	1150	5.71	0.057
24	Friction	51.10	9.00	0.00	0.000	225	1146	5.71	0.057
25	Plugged tee	0.00	9.00	0.00	1.500	225	1142	5.71	0.057
26	Friction	6.40	7.33	0.00	0.000	225	1142	5.71	0.057
27	Expansion	0.00	7.33	42.20	3.000	225	1142	5.71	0.057
28	Plug tee and bend	0.00	6.00	0.00	0.690	839	1137	5.70	0.088
29	Friction	22.40	6.00	0.00	0.000	839	1137	5.70	0.088
30	Expansion	0.00	6.00	0.00	1.750	839	1137	5.70	0.088
31	Expansion	0.00	8.00	0.00	0.544	80	389	5.90	0.048
32	Annulus	0.00	2.00	45.50	0.443	80	389	5.90	0.048
33	90 degree turn	0.00	2.00	45.50	1.200	- 80	389	5.90	0.048

TABLE 4-11
PRIMARY SYSTEM DUCT PRESSURE LOSSES FOR 2-LOOP INTERCOOLED PLANT

Item	Description (See Fig. 4-8 for Locations)	DFN (lb/cu ft)	A (sq ft)	Velocity (ft/sec)	Q (psi)	FL/D	K	ΔP (psi)	ΔP/P (%)	Sum ΔP/P (%)
1	Core	0.207	0.000	0	0.000	0.000	0.000	0.000	0.000	0.000
2	Contraction	0.207	25.518	299	2.004	0.000	0.025	0.050	0.004	0.004
3	90 degree bend	0.207	25.518	299	2.004	0.000	0.510	1.022	0.091	0.095
4	Friction	0.207	25.518	299	2.004	0.064	0.000	0.129	0.011	0.107
5	Friction	0.110	70.882	209	0.522	0.006	0.000	0.003	0.001	0.108
6	Expansion	0.110	70.882	211	0.525	0.000	3.000	1.575	0.391	0.498
7	Wye	0.190	50.266	171	0.603	0.000	0.580	0.350	0.089	0.587
8	Friction	0.190	50.266	171	0.603	0.013	0.000	0.008	0.002	0.589
9	Expansion	0.190	50.266	171	0.603	0.000	1.000	0.603	0.153	0.742
10	Contraction	0.269	50.266	121	0.426	0.000	0.335	0.143	0.037	0.778
11	90 degree bend	0.269	50.266	121	0.426	0.000	1.670	0.712	0.183	0.981
12	Friction	0.269	50.266	121	0.426	0.024	0.000	0.010	0.003	0.964
13	Friction	0.366	28.274	159	0.991	0.009	0.000	0.009	0.001	0.985
14	Expansion	0.364	28.274	159	0.995	0.000	3.000	2.986	0.446	1.412
15	180 degree turn	0.460	37.840	94	0.440	0.000	0.589	0.259	0.039	1.451
16	Contraction	0.460	37.840	94	0.440	0.000	0.500	0.220	0.033	1.484
17	Friction	0.460	37.840	94	0.440	0.370	0.500	0.383	0.058	1.541
18	Expansion	0.460	37.840	94	0.440	0.000	0.450	0.198	0.030	1.571
19	Contraction	0.460	9.621	185	1.701	0.000	0.500	0.850	0.128	1.899
20	Friction	0.460	9.621	185	1.701	0.015	0.000	0.026	0.004	1.703
21	Annulus friction	0.626	30.430	83	0.468	0.000	0.122	0.057	0.005	1.708
22	Blockage	0.626	24.000	106	0.752	0.000	0.010	0.008	0.001	1.708
23	Expansion	0.626	24.000	106	0.752	0.000	2.150	1.617	0.141	1.849
24	Friction	0.624	63.617	40	0.107	0.051	0.000	0.005	0.000	1.849
25	Plugged tee	0.622	63.617	40	0.108	0.000	1.500	0.162	0.014	1.863
26	Friction	0.622	42.199	60	0.245	0.008	0.000	0.002	0.000	1.864
27	Expansion	0.622	42.200	60	0.245	0.000	3.000	0.735	0.064	1.928
28	Plug tee and bend	0.327	28.274	172	1.037	0.000	0.690	0.715	0.063	1.991
29	Friction	0.327	28.274	172	1.037	0.034	0.000	0.035	0.003	1.994
30	Expansion	0.327	28.274	172	1.037	0.000	1.750	1.814	0.160	2.154
31	Expansion	0.269	50.266	121	0.426	0.000	0.544	0.232	0.060	2.213
32	Annulus	0.269	45.500	134	0.520	0.000	0.443	0.231	0.059	2.272
33	90 degree turn	0.269	45.500	134	0.520	0.000	1.200	0.624	0.161	2.433

$\Sigma(\Delta P/P) = 2.43\%$

With the previously described changes incorporated into the primary system layout, acceptable duct losses would result. The losses shown in Table 4-10 reflect these changes, and the pressure loss value of 2.43% has been factored into the cycle performance calculations.

4.3.3 Heat Exchanger Pressure Losses

The heat exchangers have not been optimized for minimum pressure loss, but some of the related geometry trade-offs are included in Section 4.1. Reduction in the recuperator loss, from the current 2.5% value, could be realized by increasing the cavity diameter; however, this would impact directly on PCRV diameter and is not recommended. With design refinement, it is possible that the precooler and intercooler losses could be reduced slightly, but at present these projected reductions have not been included in the analysis.

4.3.4 System Pressure Loss Summation

A summary of the system pressure losses is shown in Table 4-12. On a direct summation basis (i.e., $\Sigma\ \Delta P/P$), the losses for the 2-loop intercooled plant are 10.6%, which compares with a value of 7.15% for the 3-loop nonintercooled reference plant. If the 2-loop intercooled plant is to be further developed, a concentrated effort should be made (by cycle parameter optimization and component design refinement) to minimize system pressure losses.

TABLE 4-12
COMPARISON OF COMPONENT EFFICIENCIES AND LOSSES FOR 3-LOOP NONINTERCOOLED REFERENCE PLANT AND 2-LOOP INTERCOOLED PLANT VARIANT

Plant	3-Loop Nonintercooled	2-Loop Intercooled
Turbomachinery		
Compressor pressure ratio	2.50	3.0 (1.732/1.732)
Compressor stages	18	8 + 8
Compressor efficiency, %[(a)]	89.8	90.8 LP, 90.2 HP
Turbine stages	8	9
Turbine efficiency, %[(a)]	91.8	92.2
Cooling flow, %	3.6	3.8
Generator efficiency	98.8	98.8
Heat Exchangers		
Recuperator effectiveness	0.898	0.898
Precooler effectiveness	0.972	0.959
Intercooler effectiveness	---	0.936
System Pressure Losses ($\Delta P/P$), %		
Turbomachine inlets and exits		
Compressor inlet	0.25	0.51
Compressor exit	0.73	1.46
Turbine inlet	0.36	0.48
Turbine exit	0.46	0.40
Turbomachine losses	1.80	2.85[(b)]
Recuperator (HP side)	0.62	0.8
Recuperator (LP side)	1.22	1.2
Precooler	0.99	1.4
Intercooler	---	1.0
System duct losses	1.41	2.43
Core loss (10 row block)	1.11	0.92
Primary system loss summation[(c)]	7.15	10.60
System $(\Delta P/P) = (1 - \frac{Rt}{Rc}) \times 100$, %	6.72	10.03
Cycle efficiency (15°C ambient)	39.55	41.23

[(a)] Defined as adiabatic efficiency across blading.

[(b)] Reduction in losses felt to be possible with relaxation of design constraints (i.e., turbomachine and cavity diameters).

[(c)] Not strictly additive, but shown for comparison purposes.

REFERENCES

1. "Gas Turbine HTGR Program, Quarterly Progress Report for the Period Ending December 31, 1976," U.S. ERDA Report GA-A14243, General Atomic Company, January 1977.
2. "Gas Turbine HTGR Program, Quarterly Progress and Task Closeout Report for the Period Ending September 30, 1976," U.S. ERDA Report GA-A14097, General Atomic Company, October 1976.
3. "Gas Turbine HTGR Program, Semiannual Progress Report for the Period Ending January 1, 1976, through June 30, 1976," U.S. ERDA Report GA-A13950, General Atomic Company, July 30, 1976.
4. Rosenwasser, S.N., W.R. Johnson, and S. Liang, "Gas Turbine and Advanced HTGR Materials Screening Program, 10,000 Hour Results and Semiannual Progress Report for the Period Ending March 31, 1977," GA-A14407, June 1977.